学位論文

Microscopic method for airborne coarse particles: Application to a passive sampler

(顕微鏡観察を用いた空気中粗大粒子の測定：パッシブ型捕集装置への応用)

山本　尚理

Doctoral Thesis

Microscopic method for airborne coarse particles: Application to a passive sampler

Thesis Advisor: Professor Yukio Yanagisawa

Submitted by:

Naomichi Yamamoto

March 2006

Environmental Process Engineering Track
Course of Environment System
Institute of Environmental Studies
Graduate School of Frontier Science
The University of Tokyo

A thesis submitted to the faculty of the University of Tokyo in partial fulfillment of the requirements for the degree of Ph.D. in Environmental Studies

Contents

Acknowledgements

The present thesis is based on the research work conducted during last four years at Yanagisawa Laboratory, Course of Environment System, Institute of Environmental Studies, Graduate School of Frontier Science, the University of Tokyo.

For the completion of this thesis, I would also like to express my sincere gratitude to Prof. Yukio Yanagisawa, Institute of Environmental Studies, the University of Tokyo, who instructed me to move in the right direction of this doctoral research as a thesis advisor. I would like to express my gratitude to the members of thesis committee, Prof. Kazuhiko Sakamoto at Saitama University, Prof. Toru Sato at the University of Tokyo, Dr. Osamu Endo at the National Institute of Public Health, and Prof. Jun Yoshinaga at the University of Tokyo.

I would like to acknowledge Prof. Jun Yoshinaga, Prof. Akihiro Yamasaki at the National Institute of Advanced Industrial Science and Technology, Prof. Kazukiyo Kumagai at the University of Tokyo, and Dr. Minoru Fujii at the National Institute for Environmental Studies for providing lots of invaluable advises in the laboratory. I would like to thank Ms. Noriko Kawana, Ms. Chiyoko Kiguchi, Ms. Keiko Kawabuchi at the University of Tokyo for conducting administrative works related to my doctoral research. Furthermore, I would like to acknowledge all of the colleagues in the laboratory.

I would like to express my thanks to Dr. Derek G. Shendell at the Community Action to Fight Asthma California, Dr. Osamu Endo, Dr. Yohei Shinozuka at the University of Hawaii at Manoa for willingly collaborating with my research. Thanks are also due to Mr. Masaji Hikono, Mr. Hiromi Koyama, Mr. Mitsuru Niizeki, Pres.

Acknowledgements

Masatoshi Shibata at Sibata Scientific Technology Ltd., and Mr. Masaru Maruki, Pres. Yukiaki Tsuji, former Pres. Seiichi Miyamoto at Oji Scientific Instruments for conducting collaborative research with us.

This doctoral research was supported by the grant from the 21 Century COE Program, Ministry of Education, Culture, Sports, Science and Technology, Japan, through the Graduate School of Engineering at the University of Tokyo, the Sasakawa Scientific Research Grant from the Japan Science Society, the grant from the Suzuki Foundation, and the grant from the Steel Industry Foundation for the Advancement of Environmental Protection Technology, Japan. The author received the Travel Grant from the University of Tokyo to participate in the 3rd Asian Aerosol Conference, Hong Kong, China, too.

Finally, I would like to express my sincere appreciation to my dear parents for their unlimited support.

March 2006

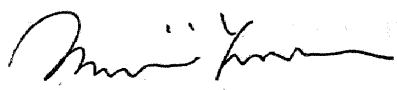

Naomichi Yamamoto

Summary

Chapter 1. Introduction

Airborne coarse particles, which are larger than 2.5 μm in diameter, are important since they include aeroallergens that can induce allergic airway diseases. Among various types of instrumental methods for airborne coarse particles, the time-integrated methods are commonly used to integrate particle mass on the substrates to provide the average mass concentration over a period ranging from minutes to days. Nevertheless, these methods tend to require long-term samplings to collect sufficient particle amounts for subsequent gravimetric or chemical analyses. While the direct-reading instruments such as light scattering particles counters (PC) are relatively sensitive, these instruments are incapable of analyzing aerosol species. Meanwhile, the microscopic methods are sensitive compared to existing gravimetric methods because they can detect individual particles. Furthermore, their advantage lies in ability to identify aerosol species by directly observing particle size and shape although the microscopic methods for determining particle size distributions are generally tedious and less precise. To overcome these difficulties, the optical microscope (OPM) with an image analysis software and line-sensing mechanism was used in this research. The purposes of this thesis are to suggest basic aspects of the OPM (Chapters 2-5) and to develop the personal aeroallergen sampler (PAAS), a passive sampler for airborne coarse particles, as an application method of the OPM (Chapters 6 and 7).

Chapter 2. Line-sensing optical microscope DA-6100LA (OPM)

The optical microscope (OPM) originally used to evaluate paper-manufacturing processes was newly employed to observe airborne coarse particles. Using its line-sensor camera with a linear motor actuating slide, broad range microscopic observation (approximately 5.5 mm × 16.2 mm) is capable at a time.

Chapter 3. Comparison of the OPM with a direct-reading method

Particle size distributions obtained by the OPM were compared with those by the PC. The particles collected on the filter surface areas of 170-420 mm^2 (18-44 % of effective areas of filtration of the 47-mm filters) were observed by the OPM. The concentrations by the OPM were correlated well with those by an existing direct-reading method, i.e., PC, indicating the measurement ability by the OPM was

comparable to that by the existing method. Furthermore, the OPM was found to be more advantageous in terms of particle sizing trueness since it permits direct measurement of particle geometrical properties and does not rely on measuring indirect properties such as light scattering. In general, twenty to thirty minutes were required to analyze the particles collected on a filter although it was dependent on the surface areas observed. The reduction of the time required to analyze sufficient number of the particles by the OPM could provide opportunities for precise and sensitive particle concentration measurements.

Chapter 4. Comparison of the OPM with existing time-integrated methods

Although the direct-reading instruments are convenient to measure the particle concentrations instantaneously, these instruments cannot analyze aerosol species. Instead, the time-integrated methods are generally used for chemical or biological analyses. For instance, the cascade impactor (CI), a type of time-integrated samplers, can collect airborne particles by particle size for subsequent size-segregated chemical or biological analyses. Nevertheless, particle size fractionation capability is known to be deteriorated by particle bounce and/or reentrainment from the impactor substrates. In this chapter, the particles collected on the impactor substrates were observed by the OPM to indicate alteration of the particle size fractionation characteristics by particle bounce and/or reentrainment from the substrates. Moreover, detection sensitivity by the OPM was exemplified in this chapter. For instance, we roughly calculated 5.2 μg of the particles were lost from the non-greased substrates. Since a practical limit of the sensitivity for weighing most air-sampling filters by microbalances is generally 10 μg, it is apparent the OPM is sufficiently sensitive to analyze the particle size distributions well below the detection limits of the microbalances. In this chapter, sensitivity of the OPM was demonstrated by comparing that by a direct weighing method by an analytical microbalance, too.

Chapter 5. Summary of the OPM

The sensitivity of the OPM method, which was clarified in Chapters 2-4, can decrease the required amounts of the particles for subsequent gravimetric or chemical analyses. In accordance, the sampling time and rate can be reduced. The reduction of the sampling time creates opportunities of the time-resolved particle concentration measurements while the decrease of the sampling rates is ultimately attained to the passive sampling methods.

Chapter 6. Development of the PAAS

In Chapter 6, general features of the PAAS as well as its significance were discussed. Although it is generally difficult for the passive samplers to collect adequate amounts of the particles for subsequent gravimetric or chemical analyses, the OPM is expected to be sufficiently sensitive to quantitate the amounts passively collected. As one of characteristic features of the PAAS, a gimbal-like structure was adopted for the substrate holder to enable the particle collection substrate to be continuously directed upward regardless of inclination of the sampler. Moreover, the PAAS was designed to collect airborne particles proximate to the human breathing area by wearing it around his or her neck.

Chapter 7. Evaluation of the PAAS-OPM

The particle collection characteristics by the PAAS were evaluated by the OPM. Specifically, the particle size distributions obtained by the PAAS were compared with those by an existing active sampler, i.e., the IOM sampler. The results showed good correlations between the two methods, suggesting usability of the PAAS for long-term personal monitoring of coarse airborne particles including aeroallergens. The particle collection velocities onto the PAAS were lower than those theoretically calculated based on an existing dry deposition model. The lower experimental values were expected due to the effects of the sampler's geometry. Unlike existing active samplers, the PAAS is convenient for personal air monitoring because of its simplicity of handling. Therefore, it can be used for a variety of epidemiological surveys to investigate relationships between the aeroallergen exposures and allergic airway diseases.

Chapter 8. Overall summary and conclusions

The detection sensitivity of the OPM method can provide opportunities of the time-resolved and passive-sampling analyses for airborne particles. In this thesis, a passive sampler for coarse airborne particles, i.e., the PAAS, was developed to exemplify an application method of the OPM. The detailed mechanisms of allergic airway diseases can be elucidated by using the PAAS in large-scale epidemiologic investigations.

Summary (in Japanese)

第 1 章　序言

比較的長期にわたり空気中に浮遊した状態で存在することの出来る粒子を浮遊粒子状物質と呼ぶ。粒径 2.5 μm 以下の微小粒子による健康影響が懸念される一方、粒径 2.5 μm 以上の粗大粒子もアレルギー疾患の原因となる吸入性アレルゲン(ダニの糞: 10-40 μm、真菌胞子: 2-60 μm、スギ花粉: 25-60 μm)を含んでおり、重要な粒子種といえる。浮遊粒子状物質の定量手法として、基質に捕集した粒子全体を秤量し、質量濃度として評価する手法がこれまで一般的であった(時間積分型)。しかしながら、これらの手法では対象物質の量が必要となることから、捕集の長期化や動力源の確保など問題点も多かった。光散乱式パーティクルカウンター(PC)など高感度な直読型の測定装置も存在するが、対象物質の保存が利かないことから、粒子種の定性が行えないなどの欠点を持つ。一方、顕微鏡観察は、高感度なことから、既存手法では検出不可能な領域にて粒子の個数濃度の解析が可能であり、観察した粒子の密度や形状係数を仮定することで質量濃度への換算も可能である。また、免疫染色などの手法を用いることで粒子種の定性も行える。しかしながら、顕微鏡観察法は、手間がかかることや精度の問題が指摘されている。本研究では、ラインセンサーや画像解析機能を備えた光学顕微鏡(OPM)を用いることで、測定精度の向上や解析時間の短縮を試みた。本論文の前半部(第 2-5 章)では、OPM による粒子解析手法の特徴について、既存手法であるカスケードインパクター(CI)(時間積分型)や PC(直読型)と比較することで明らかにした。本論文の後半部(第 6、7 章)では、OPM の特徴を活用した携帯型アレルゲン捕集装置(PAAS)を開発することで、OPM の発展性について例示することにした。

第 2 章　OPM の概要

製紙プロセスにおける異物評価や印刷評価に用いられてきた OPM を、濾紙上に捕集した粒子の評価に用いることにした。リニアステージの移動とともにラインセンサーカメラにより顕微鏡画像を取り込むことから、既存の顕微鏡と比較し、観察視野の確保が容易である。また、顕微鏡画像は、付属の画像解析ソフトにて粒径分布の解析が可能である。

第 3 章　OPM と直読型測定装置の比較

OPM による粒径分布の定量について、既存手法である PC と比較することで評価した。PC により粒子濃度をリアルタイム測定すると同時に、粒子をフィルター捕集した。

捕集フィルターは、OPM にて 170-420 mm^2 の範囲(有効濾過面積の 18-44 %)をランダムに観察することで粒子数および粒径を定量した。また、OPM の粒径定量の真度について、標準粒子を観察することで評価した。両手法間に正の相関があることを確認したが、OPM にて定量した粒径分布は PC にて定量したものと比較し、粗大側に位置することが分かった。Mie 散乱理論により PC にて定量した粒径を補正した結果、PC の粒径は光散乱径として表現されることから、OPM にて得られる投影径と異なることが示唆された。OPM の特徴として、(1)PC と比較し遜色ない粒子個数の測定が可能なこと、(2)粒子の光散乱特性を利用して粒径定量を行う PC と比較し、粒子を直接観察することから粒径定量の真度が高いこと、が分かった。

第 4 章　OPM と時間積分型測定装置の比較

PC は粒径分布を簡易に測定可能な一方、直読式であることから、粒子の保存が利かない。したがって、粒子種の定性を行えないなどの欠点を持つ。粒子を粒径ごとに捕集可能な手法として、慣性力により分級を行う CI がある。しかしながら、慣性力の大きな粗大粒子は慣性衝突時に基質から跳ね返るなどの問題がある。本章では、CI の分級性能や時間積分型装置全般におけるの測定感度の問題点について、OPM にて評価した。CI の捕集基質としてテフロン基質をインパクターノズル(分級範囲 >7.0 μm)の真下に装着し、45 分間の粒子捕集を行った。基質はグリースを塗布したものとそうでないものを用い、捕集後の基質は OPM にて解析した。また、濾過法によって捕集した粒子を、可読性 0.1 mg の電子天秤および OPM にて定量した。単位密度の球形粒子を仮定した場合、5.2 μg 相当の粒子がグリースを塗布していない捕集基質から損失していることが計算された。高速ノズルにより粒子を慣性衝突捕集することから、基質上での跳ね返りによる損失が原因として考えられる。また一般的に、CI や濾過法にて捕集した粒子は、電子天秤により定量されるが、その検出感度が 10 μg 程度であることを考えると、OPM がいかに高感度な手法であるかが分かる。CI の問題点として、(1)粒子の跳ね返りにより分級性能が低減すること、(2)粒径定量が不正確なこと、が確認出来た。また OPM の特徴として、(3)高感度なこと、が分かった。

第 5 章　OPM のまとめ

OPM の特徴として、(1)高感度なこと、(2)十分な粒子個数の測定が可能なこと、(3)解析時間の短縮が可能なこと(観察面積にも依るが、1 検体あたり約 20-30 分程度)、(4)粒径定量の真度が高いこと、が確認出来た。以上の特性を応用することで、粒子の時間分解解析やパッシブ型捕集装置への応用が期待される。

第 6 章　PAAS の開発

これまでポンプなど動力を利用したアクティブ型の捕集装置が浮遊粒子状物質の

個人曝露評価で用いられてきたが、重量、騒音、電力の必要性などから不便であることが指摘されてきた。そこで本研究では、ポンプを用いないパッシブ型の捕集装置を開発することにした。粗大な吸入性アレルゲンを捕集対象とすることから、粒子の重力沈降を捕集の駆動力として想定している。そこで、被験者の動きによらず、粒子捕集面が常に上向きとなるよう、回転可能なジンバル型の捕集装置とした。また、被験者の呼吸域近傍にて捕集可能なよう、首からぶら下げるためのステンレス鎖を取り付けた。捕集した粒子はOPM観察により粒径情報が得られることから、捕集粒子量から空気中濃度への換算が可能となる。また、粒子を免疫染色した後、顕微鏡観察することでアレルゲン種の定性が行える。

第7章 PAAS-OPMの評価

PAASの粒子捕集性能について、既存のアクティブ型捕集装置と比較することで評価した。捕集粒子はOPMにて個数および粒径を定量した。PAASおよび既存のアクティブ型装置であるIOM Samplerによる粒子の同時捕集を行った。また、捕集基質としてメンブレンフィルターを用いた。粒子捕集は、室外および個人曝露の条件下にて、5-150 hrの捕集時間で行い、捕集後の基質はOPMにて解析した。パッシブ型およびアクティブ型装置によって捕集した粒子数に、概ね良い相関を確認することが出来た。従って、PAAS による捕集粒子量より、正確な個人曝露濃度の算出が可能と思われる。また、PAASの粒子捕集速度について、既存の乾性沈着モデルから予想される理論速度と比較したところ、過小な値をとることが分かった。PAASの形状に起因するものと思われる。実験結果より、粒子の捕集速度V_dをモデル化したところ、V_d=0.28V_gとなる回帰式により表されることが分かった。ここでV_g: Stokes沈降速度。PAASの特徴として、捕集量から空気中濃度への換算が可能なことが分かり、またPAAS-OPMの特徴とし、高感度なOPMを解析手法として用いることでパッシブ捕集した微量試料から正確に濃度定量が行えることが分かった。

第8章 結言

OPMを応用することで、吸入性アレルゲンを含む浮遊粒子状物質の時間分解解析が可能と思われる。また、PAAS-OPMを用いることで、正確かつ簡易な吸入性アレルゲンへの曝露評価が可能である。広範かつ精緻な曝露評価を可能とすることで、未解明な部分も多かったアレルギー疾患の詳細に関し、新たな知見を付与することが期待される。

List of Tables

List of Figures

List of Abbreviations

ACGIH	American Conference of Government Industrial Hygienists
CI	cascade impactor
EDX	energy dispersive X-ray fluorescence
ELISA	enzyme-liked immunosorbent assay
G	greased substrate
GSD	geometric standard deviations
IC	ion chromatography
IgE	immunoglobulin E
IOM	Institute for Occupational Medicine
MCE	mixed cellulose ester membrane
MLI	Multistage Liquid Impinger
MOUDI	Micro-Orifice Uniform Deposit Impactor
NG	non-greased substrate
NIOSH	National Institute for Occupational Safety and Health
NIST	National Institute of Standards and Technology
NOx	nitrogen oxides
OPM	optical microscope
PAAS	Personal Aeroallergen Sampler
PC	light scattering particle counter
PCM	phase-contrast microscopes
PM2.5	particles with diameters smaller than 2.5 μm
PM10	particles with diameters smaller than 10 μm
RH	relative humidity
SAS	Surface Air System Sampler
SD	standard deviation
SE	standard error
SEM	scanning electron microscope
TEM	transmission electron microscope
VOCs	volatile organic compounds
XRF	X-ray fluorescence spectroscopy

List of Principal Symbols

a	parameter related to the sampler's geometry
A	surface area of the substrate
A_e	effective particle deposition area
C	particle number concentration
C^*	particle size conversion factor
C_c	Cunningham correction factor
d	particle diameter
d_a	particle aerodynamic diameter
d_e	particle equivalent volume diameter
d_{OPM}	particle diameter measured by optical microscopes
d_{PA}	particle projected area diameter
d_{PC}	particle diameter measured by light scattering particle counters
d_{PC^*}	theoretical geometric particle diameter inferred by particle counter observation
D_j	impactor jet diameter
F	particle number flux
g	acceleration of gravity
IF	inhalable fraction
m	refractive index; mass of particle
m_{cal}	calibration refractive index
m_{meas}	refractive index of measured particles
n	particle numbers on a unit area; number of samples
n_0	true number of particles
n_a	particle numbers on a unit area of a collection substrate of an active sampler
n_p	particle numbers on a unit area of a collection substrate of a passive sampler
N	number concentration; number of particles
Q	flow rate
R^2	squares of the correlation
s	angular scattering intensity
$\mathrm{Stk_e}$	eddy Stokes number
t	time

u^*	friction velocity of air
U_0	ambient air velocity
v	kinematic viscosity of air (= 0.156 cm^2 s)
V_0	face velocity of air
V_d	particle dry deposition velocity
V_g	particle terminal settling velocity
V_i	particle inertial velocity
v_p	particle volume
α_v	volume shape factor
η	air viscosity (= 1.8×10^{-5} Pa s)
η_{dI}	eddy deposition efficiency
θ	scattering angle
λ	wavelength
ρ_0	standard density (= 1000 kg m^{-3})
ρ_p	particle density
χ	dynamic shape factor

CHAPTER 1.
Introduction

CHAPTER 1. Introduction

1.1. Natures of airborne coarse particles

1.1.1. Physical, chemical and biological properties

Airborne particulate matters, microscopic substances floating in the air, include resuspended soil, smoke from power generations, photochemically formed substances, salt formed from ocean spray, and atmospheric clouds of water droplet or ice particles, and so on (Hinds, 1999). Airborne particles have various diameter ranges from molecular clusters to ~100 μm (Finlayson-Pitts & Pitts, 2000). Atmospheric fates and behaviors of the particles are determined by their size, shape and density. While the Brownian diffusion, irregular wiggling motion of the particles in the air by the persistent collision of gas molecules, is a predominant mechanism for fine submicron particles, gravitational settling plays an important role for coarse micrometer-sized particles, since terminal velocity of the particles due to gravitational settling, V_{TS}, is increased to the second power of the particle size, and given by a following equation:

$$V_{TS} = \frac{\rho_p d_a^2 C_c g}{18\eta}, \qquad (1.1)$$

where ρ_p is the particle density, d_a is the particle aerodynamic diameter, C_c is the Cunningham correction factor, g is the acceleration of gravity, and η is the air viscosity. In consequence, atmospheric lifetimes of the particles significantly vary depending on their sizes. For instance, while the fine particles smaller than 2.5 μm in diameter have lifetimes of days in troposphere, the particles larger than 20 μm are removed in a matter of hours (Hinds, 1999). Therefore, the large particles settle out of the atmosphere by sedimentation, except on windy days, where fallout is balanced by reentrainment.

Turbulent deposition is also important for airborne coarse particles. In this mechanical process, the particles with aerodynamic diameters larger than about 1 μm deposit to a surface because of the fluctuating velocity components of a turbulent gas carrying the particles (Friedlander, 2000). It is known that deposition velocities due to turbulence are strongly dependent on the particle diameter and gas velocity.

It should be stated the aerodynamic diameter was not an actual particle size such as characterized by microscopic observation. Instead, the aerodynamic diameter of the particle is defined as a diameter of a spherical particle having the standard density (= 1000 kg m^{-3}) that has the same settling velocity:

$$d_a = d_e\left(\frac{\rho_p}{\rho_0 \chi}\right)^{0.5}, \qquad (1.2)$$

where d_e is the equivalent volume diameter, χ is the dynamic shape factor, ρ_0 is the standard density (= 1000 kg m^{-3}).

In general, each chemical component is found in specific size ranges depending on the sources of each particle having specific size ranges (Finlayson-Pitts & Pitts, 2000). For instance, ultrafine particles with diameters less than 0.01 μm are produced by homogeneous nucleation and hence tend to contain secondary species such as sulfate and organics. The particles in the Aitken nuclei range with diameters of 0.01-0.08 μm, on the other hand, are produced by combustion processes, coagulation of the smaller particles, and condensation of low-vapor-pressure products of gas-phase reactions. Therefore, these particles tend to contain elements such as carbon and some trace metals including V, which are characteristics of combustion, as well as sulfates, nitrates, and polar organics. Meanwhile, coarse particles, which are larger than 2.5 μm in diameter, typically contain elements in soil, salt, and so on because mechanical processes such as

grinding, wind, or erosion are primarily responsible for these particles. Moreover, majority of biological particles tend to be in the coarse size range. For instance, mite fecal pellets, cedar pollens and fungal spores have diameters of 10-40, 25-60 and 2-60 μm, respectively (Tovey et al., 1981; Kitamura, Shiomori et al., 2005; Al-Doory & Domson, 1984). Furthermore, biological particles can be divided into two main categories, i.e., viable and nonviable. Viable bioaerosols are living microorganisms that can be identified and quantitated by growing individual organisms with suitable nutrients into visible clusters or colonies. These microorganisms include bacteria, fungi, viruses, algae and so on. Meanwhile, nonviable bioaerosols include dead microorganisms, pollens, animal hair and dander, fragments and excreta from dust mites and cockroaches, and saliva and dander from dogs, cats and birds.

Among various types of bioaerosols, aeroallergens are those immunological. Immunological bioaerosols including human and animal hair and dander, mites, molds, pollens, textiles, food leftovers, bacteria, insect parts and decomposed materials (Lowenstein et al., 1986) are important in view of respiratory allergic diseases. Among various types of aeroallergens, house dust mite is one of major allergenic substances (Platts-Mills & Chapman, 1987). Bed dust tends to be the most potent source for dust mite allergen, and greatest exposure to airborne dust mite allergen is known to occur in the bedroom. Allergen-rich dust mite fecal particles with diameters of 10-40 μm are thought as major house dust allergens (Tovey et al., 1981). Since these allergenic particles are relatively large in size, they are in air only shortly after the disturbance and settles rapidly due to gravitation. Aeroallergens of animal origins are also common problems in clinical allergy because of high prevalence of keeping furred animals as pets. Cat allergenic extracts are particularly well-characterized allergens of

animal origins. *Fel d* I, a major cat allergen, is one of ten potentially allergenic components of cat extract (Ohman et al., 1974; Lowenstein et al., 1985). While cat antigen levels increases remarkably during dust disturbance period (Swanson et al., 1985), resuspended *Fel d* I is known to remain airborne for prolong periods and observed even in undisturbed houses. Fungi are known allergens (Achatz et al., 1995; Bush & Portnoy, 2001; Jacob et al., 2002) often contained in house dust (Korpi et al., 1997) even in the absence of environmental mold (Becker et al., 1996). Airborne fungal spores ranging 2-60 μm in diameter (Al-Doory & Domson, 1984) are important to cause allergic rhinitis or asthma (Achatz et al., 1995; Kurup et al., 2000). Cedar pollens are another aeroallergens known to cause pollinosis accompanied with symptoms such as allergic rhinitis and conjunctivitis, and rarely with allergic asthma and dermatitis. Grains of cedar pollens range 25-60 μm in diameter (Kitamura et al., 2005).

1.1.2. Health effects

Airborne coarse particles generated from mechanical processes such as grinding, wind, or erosion, are generally non-toxic since they usually contain inert substances from soil, salt, and so on. While epidemiological studies have shown a relationship between exposures to fine particles with diameters less than 2.5 μm (PM2.5) and community health effects (Dockery et al., 1993; Schwartz et al. 1996), no studies have ever proven adverse health effects caused by the coarse particles. Nevertheless, the coarse particles are important since a majority of bioaerosols that can be immunological is in the coarse size range. Allergic reactions including asthma and/or rhinoconjunctivitis are known to be induced by inhalation of allergenic particles

such as dust mite fecal pellets, fungal spores, cedar pollens, and so on. At present, approximately 40 to 50 million people in Japan are known to have any types of allergic symptoms. For example, asthma-related medical expenditure including indirect expenses such as economic loss due to work-day lost was approximately 640 billion yen in Japan in 2000. Meanwhile, approximately 13 million people are thought to suffer from cedar pollinosis, a sort of allergic rhinitis caused by inhalation of cedar pollens, while annual economic losses due to cedar pollinosis are estimated to be 290 billion yen. More importantly, the economic loss due to allergic airway diseases is still on the increasing tendency. For instance, annual medical expenditure due to allergic asthma has increased by 148 billion yen from years 1990 to 2000. Thus, issues related to allergic diseases have to be urgently solved from the economic and public welfare aspects.

Allergic reactions such as asthma and/or rhinoconjunctivitis are induced when allergens, foreign proteins such as aeroallergens, elicit an immune reaction involving B and T cells. Briefly, immunoglobulin E (IgE) produced by B cells as a result of contact of allergens with allergen-presenting cells binds to surface receptors present on a wide variety of cells, most importantly mast cells and eosinophils (Corry & Kheradmand, 1999). Cross-linking of IgE with the receptor during subsequent encounter with allergens stimulate release of a variety of toxic products (e.g., histamine, leukotrienes, prostaglandins, cytokine) that together elicit allergic reactions (Corry & Kheradmand, 1999). While the mechanisms of allergic reactions have been clarified to a considerable degree, detailed mechanisms of the disease expression are not completely understood partly because various environmental factors, e.g., tobacco smoke, air pollutants and infections, are also known to be associated with the disease expression.

Therefore, interactions between the exposures to inhalant allergens and non-specific adjuvant factors, e.g., air pollutants, have to be better understood to clarify their effects. To elucidate abovementioned interactions among various environmental factors against the disease expression, accurate assessments of the personal exposures to inhalant aeroallergens in conjunction with those to other environmental factors are essential. Consequently, accurate and simplified methodologies to assess the personal exposures to inhalant aeroallergens are highly desirable for extensive uses for the epidemiologic researches.

1.2. Existing methodologies for airborne particles

Among many methods for aerosol analyses, there are two types in general, time-integrated and direct-reading methods. In the time-integrated methods, the filter or substrate samples integrate particle mass to provide the average aerosol concentrations over a period ranging from minutes to days. Using a microbalance, collected particles on a filter are gravimetrically analyzed by weighing the filter before and after the air sampling. There are two types of the time-integrated methods, i.e., active and passive methods. While the active samplers are those operated with pumps, the passive samplers collect airborne particles by naturally occurred mass transfers. In general, the time-integrated filter sampling methods are simple, low-cost, and widely used to accurately determine average mass concentrations. Furthermore, chemical components included in the particles collected on the filters or substrates can be analyzed by chemical constituent analyses such as X-ray fluorescence spectroscopy (XRF) for metal species, thermal/optical analyses for elemental and organic carbons, and ion chromatography (IC) for ionic species such as nitrates or sulfates.

Nevertheless, the methods require long-term sampling durations to achieve sufficient amounts of the particles for subsequent gravimetric and/or chemical analyses. Although direct-reading instruments can measure mass concentration in a few minutes at the sampling site by measuring particle properties such as light scattering, light absorption, mechanical mobility, or electrical mobility, they are less accurate than gravimetric filter measurements and generally incapable to analyze chemical compositions.

1.2.1. Time-integrated methods

Filtration is a commonly used active sampling method to collect airborne particles. Among various types of the filters commercially available, fibrous and porous membrane filters are the most common types for aerosol filtration. In filtration methods, airborne particles in flowing air are captured by microscopic structures of the filters. Although there is still a gap between the theory and experiment in terms of particle collection by filtration, the general principles are well understood (Hinds, 1999). For instance, Yamamoto et al. (2004, 2005) assumed gravitational settling, impaction, interception, and the Brownian diffusion as particle collection mechanisms for capillary pore membrane filters and Nylon mesh filters, respectively (see Appendixes A2 and A4). Filtration is used to collect airborne coarse particles such as aeroallergens, too. For instance, Palmgren et al. (1986) used Nuclepore filters to collect airborne microorganisms. In their study, the collected microorganisms are washed off from the filters to culture the viable microorganisms while those non-viable were stained and enumerated by an epifluorescence microscope.

Inertial impactors that can collect airborne particles on the sampling substrates

by accelerating air to hit particles on the substrates by means of inertia are used to collect airborne particles, too. An advantage of the impactors lies in ability to fractionate the airborne particles by size. For instance, the Andersen sampler (Andersen, 1958), a type of cascade impactors, collects airborne particles onto a series of nutrient agar plates to obtain the particle size distribution information within the sampled aerosols. Meanwhile, the Casella Slit Sampler (Bourdillon et al., 1941) samples air at high speed through narrow slits onto a rotating nutrient agar plate while the Surface Air System Sampler (SAS), a portable single-stage sieve sampler, collects particles onto an agar filled Rodac plate (Lach, 1985). The impingers operate much like an impactor except that the jet is immersed in water or alcohol. In these methods, airborne particles are captured by inertial mechanisms and end up suspended in a liquid. An advantage of the impingers lies in ability to prevent desiccation of the microorganisms by liquid collection. Another types of commonly used impactors and impingers include the Cyclone (Errington & Powell, 1969), the Porton All Glass Impinger (May & Harper, 1957), and the Multistage Liquid Impinger (MLI) (May, 1966).

In general, the active sampling methods are suitable to collect sufficient amounts of the particles for subsequent gravimetric or chemical constituent analyses. Meanwhile, the active methods are often impractical for long-term personal air samplings due to limited lifetime of battery, noise, weight of pumps, and dimensions of the samplers.

1.2.2. Direct-reading methods

Direct-reading instruments such as light scattering instruments (Kerker, 1997),

time-of-flight monitors (Cheng et al., 1993), condensation nuclei counters (Agarwal & Sem, 1980) and electrical mobility analyzers (Flagan, 1998) allow us to measure particle concentrations in a few minutes. Because of their capability to instantaneously measure the particle concentrations at the monitoring sites, direct-reading instruments have been widely used in occupational hygiene surveys or clean room control systems for continuous and periodical detection of airborne particles. Although direct-reading instruments are convenient in such monitoring situations, they are occasionally less accurate because they rely their measurement on measuring indirect properties of the particles such as light scattering, light absorption, mechanical or electrical mobility (Hinds, 1999). Furthermore, the direct-reading instruments often involve complicated operation procedures, and these instruments often require delicate handling and transportation, which makes frequent relocation of the monitoring points difficult. More importantly, limitation of the direct-reading instruments lies in inability to preserve the measured particles for subsequent chemical constituent analyses.

1.2.3. Analytical methods

1.2.3.1. Bulk methods

The gravimetric analysis is the most commonly used method for determining mass concentrations of airborne particles. In this method, filters or substrates on which the aerosol particles are collected are weighed by microbalances before and after the air samplings. The mass of the particles collected on a filter or substrate is calculated by subtracting the mass of the filter or substrate before and after the sampling. Hereafter, the difference is divided by the sampled air volume to calculate the particle concentration in air for the periods of the sampling. Usually, an analytical balance or

an electrobalance is used to weigh the filters or substrates. While the analytical balance is a mechanical beam balance having sensitivity of 0.1 mg, the electrobalance is more sensitive using the torque on the coil in a magnetic field to balance a mechanical beam. In general, sensitivity ranges from 0.1 μg on the most sensitive scale to 10 μg on the least sensitive scale. For weighing most air-sampling filters, 10 μg is a practical limit of sensitivity (Hinds, 1999).

As described above, chemical components of the particles collected on the filters or substrates can be analyzed by XRF for metal species, thermal/optical analyses for elemental and organic carbons, and IC for ionic species including nitrates or sulfates. As is the case with the gravimetric analysis, sensitivity of each analytical method has to be well recognized to determine appropriate sampling durations to achieve sufficient amounts of the sampled particles for subsequent chemical constituent analyses. For instance, Martuzevicius et al. (2004) reported detection limits for 37-mm Teflon filters analyzed by XRF ranging 5.5 ng for cobalt, nickel and copper to 980 ng for sodium. Meanwhile, they reported the detection limit for the thermal-optical transmittance analysis for elemental carbon to be 17 μg. In their study, they sampled the urban aerosols for 24 hr to analyze the chemical constituents by the abovementioned methods.

To detect biological particles including aeroallergens, enzyme-liked immunosorbent assays (ELISA) are often used. This method uses enzymes to detect antibody molecules such as allergenic proteins. The covalent attachment of enzymes to antibody molecules creates immunological tools possessing high specificity. Among a variety of immunoassay techniques, disposable microtiter plate techniques have been most widely used. In this method, proteins, either antigens or antibodies, are adsorbed to the plastic surface of the microtiter plate. Once proteins are bound to

the surface, the plate is treated by several reagents and washed repeatedly without being removed from the plate surface. The absorbance of colored antigens on the plate surface is read by automatic plate readers. While the ELISA is known to be relatively sensitive, i.e., detection limits ranging 0.1-10 ng per sample in general, the methods involve multiple procedures in sample preparation. Furthermore, the methods require incubation for sample preparation, which usually takes time of several hours.

In general, the bulk methods are less sensitive compared to the microscopic methods for instance, and require large amounts of the target substances to be quantitated by subsequent gravimetric or chemical analyses. Consequently, long-term samplings using pump-operated active samplers, which are frequently inconvenient for the personal monitoring, are usually essential.

1.2.3.2. Microscopic methods

The microscopic methods are occasionally used to detect, count, and size the particles collected on the filters or substrates. The methods are advantageous in terms of detection sensitivity since they can observe individual particles. Therefore, detection sensitivity of the microscopic methods can be defined as quantities of each individual particle observed by the microscopes. Furthermore, the mass of the particles can be estimated by the particle size distribution observed by the microscopes with certain assumptions. For instance, the mass of the particle, m, can be given by a following equation:

$$m = \rho_p v_p = \rho_p \frac{\pi}{6} d_e^3 = \rho_p d_{\mathrm{PA}}^3 \alpha_v, \qquad (1.3)$$

where v_p is the particle volume, d_{PA} is the projected area diameter, and α_v is the volume shape factor. While the value of d_{PA} can be measured by microscopic observations, the

values of ρ_p and α_v can be retrieved from the literatures (e.g., Davies, 1979; Hinds, 1999; Tai et al., 1999; van Hout & Katz, 2004; Yang et al., 2005) although these values are partly empirical. The empirical ratios of d_a/d_{PA} are also available for mineral dusts and ambient aerosols from the literatures (e.g., Davies, 1979; Noll et al., 1988). Therefore, the conversions from the projected area diameters characterized by microscopic observations to the aerodynamic diameters are feasible with these empirical assumptions. Since various environmental standards such as PM2.5 and PM10, i.e., standards for airborne particles having aerodynamic diameters less than 2.5 and 10 μm, respectively, are based on the mass concentrations in air, the abovementioned equation can be used to convert the number concentrations characterized by microscopes to the mass concentrations used as environmental standards. Moreover, since the cleanroom standards for airborne particles are generally based on the number concentrations (e.g., ISO 14644-1 and JIS B 9920) (Fujii & Kagi, 2002), the particle number concentrations characterized by microscopic methods can be directly used for these standards without converting to the mass concentrations.

Among several types of the microscopes, optical microscopes (OPM) are most commonly used. The optical microscope uses a visible light from an external light source, in which the light reflected by a sample is collected by an objective lens to concentrate the reflected light and magnify the image of the sample. There are two types in general, reflection and transmission optical microscopes. While the reflection microscopes are suitable to observe opaque substances such as metals, the transmission microscopes are appropriate to detect transparent or translucent specimens such as animal or plant cells. Since the resolving power of optical microscopes is generally ~0.4 μm, they are usually used to observe pollens, asbestos, or airborne soil dusts,

which are generally larger than this resolution range.

Electron microscopes, on the other hand, use electron beams to capture the images of target substances. There are two types, scanning and transmission electron microscopes. In scanning electron microscopes (SEM), a surface of a solid sample is scanned in a raster pattern with a beam of energetic electrons. Transmission electron microscopes (TEM), on the other hand, shine a beam of electrons through the specimen and transmitted electrons are focused by the objective lens into an image. Several types of signals produced from the surface irradiated by electrons, such as backscattered, secondary, and Auger electrons, and X-ray fluorescence, are measured to characterize physical and chemical properties of the target substances. Although the resolving power of electron microscopes is generally high, i.e., ~0.001 μm, a limitation of electron microscopes lies in inability to observe volatile and degradable particles under the effects of high vacuuming and heating by the electron beam. Using the high resolving powers of the electron microscopes, diesel nanoparticles are often characterized by these microscopes (e.g., Lapuerta et al., 2003).

To observe biological particles that can be allergenic, fluorescence microscopes can be used (Palmgren et al., 1986). In these microscopes, cells of the microorganisms are stained with a fluorescent dye and counted directly by the microscopes. This method uses fluorochromes that can attach to particular cell components to fluoresce when excited with the light with a suitable wavelength. In these fluorescent methods, the black filters are occasionally used to produce a dark background to improve the images. To observe allergenic particles, methods using an immunoassay are useful. Using a fluorescently labeled and enzyme-linked antibody that binds to a specific antigen on the surfaces of target microorganisms, theses microorganisms can be

selectively fluorescent and observed by the fluorescence microscopes even within a background of other species. An advantage of the immunoassay methods is its selectivity to identify allergenic species. The phase-contrast microscopes (PCM) are another alternatives to observe bacterial endospores as they appear phase-bright against the darker vegetative cells. It should be stated that the PCM was also used to observe asbestos, which are transparent and hardly visible by biological microscopes. The PCM is used as reference methods for counting asbestos in Japan (Ministry of the Environment, Japan, 2005) and the U.S. (National Institute of Occupational Safety and Health, 2005).

The microscopic methods are useful to characterize particle's additional information including sizes, shapes and colors. The microscopic methods are also advantageous in terms of detection sensitivity where the gravimetric analyses are not feasible. Since the masses of spherical particles with unit density (= 1000 kg m^{-3}) having diameters of 0.1, 1, 10, 100 μm are 520 ag, fg, pg and ng, respectively, the microscopic methods can detect ag order of the particles in theory. Nevertheless, the microscopic methods for determining particle size distributions are slow, tedious and often inaccurate due to operator error or bias because investigations are usually performed manually (Hinds, 1999). In asbestos counting, for instance, only 0.4 % of an effective filtration surface of the 47-mm filter is subjected to microscopic observation (Ministry of the Environment, Japan, 2005). This inevitably causes insufficient statistical power in the counting. Moreover, since asbestos counting is known to be labor-intensive since it is performed manually, human error in counting is occasionally significant.

1.3. Overall objectives of this research

To overcome abovementioned difficulties of the microscopic methods such as insufficient statistical power as well as human error in determining the particle size distributions, we have recently introduced a novel optical microscope (OPM) consisting of a line-sensor camera in conjunction with a linear actuating slide and an image analysis software. The precise measurements of the particles collected on the substrates are expected because broad range microscopic observations as well as computer-based image analyses are capable by using the abovementioned features of the OPM. Briefly, the purposes of this research are to: (1) demonstrate usability of the OPM for the purpose of measuring airborne coarse particles (Chapters 2-5), (2) develop a passive sampler for airborne coarse particles by means of detection sensitivity of the microscopic method (Chapters 6 and 7).

In particular, the specifications of the OPM are described in Chapter 2. In Chapters 3 and 4, the basic experiments were conducted to demonstrate advantages of the OPM method for the purpose of aerosol measurements. In Chapter 5, the characteristics of the OPM method are summarized, and its future prospects were proposed. In particular, the capabilities of time-resolved and passive sampling methods were suggested. In Chapter 6, a passive sampler for airborne coarse particles, i.e., the personal aeroallergen sampler (PAAS), was developed by means of the detection sensitivity of the OPM method that was clarified in the previous chapters. In Chapter 7, the performance of the PAAS was evaluated by the OPM. In Chapter 8, overall summary and conclusions of the thesis are described. A structure of this thesis is shown in Figure 1.1.

References

Achatz, G., Oberkofler, H., Lechenauer, E., Simon, B., Unger, A., Kandler, D., Ebner, C., Prillinger, H., Kraft, D., & Breitenbach, M. (1995). Molecular cloning of major and minor allergens of Alternaria alternata and Cladosporium herbarum. *Molecular immunology, 32*, 213-227.

Agarwal, J. K., & Sem, G. J. (1980). Continuous flow, single-particle-counting condensation nucleus counter. *Journal of Aerosol Science, 11*, 343-357.

Al-Doory, Y., & Domson, J. F. (1984). *Mould Allergy*, Philadelphia, Lea and Febiger.

Andersen, A. A. (1958). New sampler for the collection, sizing, and enumeration of viable airborne particles. *Journal of Bacteriology, 76*, 471-484.

Becker, A. B., Muradia, G., & Vijay, H. M. (2001). Immunoreactive Alternaria allergens in house dust in the absence of environmental mold. *Journal of Allergy and Clinical Immunology, 97 (suppl 1)*, 151.

Bourdillon, R. B., Lidwell, O. M., & Thomas, J. C. (1941). A slit sampler for collecting and counting airborne bacteria. *Journal of Hygiene, 14*, 197-224.

Bush, R. K., & Portnoy, J. M. (2001). The role and abatement of fungal allergens in allergic diseases. *Journal of Allergy and Clinical Immunology, 107*, 430-442.

Cheng, V. S., Barr, E. B., Marshall, I. A., & Mitchell, J. P. (1993). Calibration and performance of an API aerosizer. *Journal of Aerosol Science, 24*, 501-514.

Corry, D. B., & Kheradmand, F. (1999). Induction and regulation of the IgE response. *Nature, 402*, B18-B23.

Davies, C. N. (1979). Particle-fluid interaction. *Journal of Aerosol Science, 10*, 477-513.

Dockery, D. W., Pope III, C. A., Xu, X., Spengler, J. D., Ware, J. H., Fay, M. E., Ferris, B. G., & Speizer, F. E. (1993). An association between air pollution and mortality in six U.S. cities. *New England Journal of Medicine, 329*, 1753-1759.

Errington, F. P., & Powell, E. O. (1969). A cyclone separator for aerosol sampling in the field. *Journal of Hygiene (Cambridge), 67*, 387-399.

Finlayson-Pitts, B. J., & Pitts, J. N. (2000). *Chemistry of the upper and lower atmosphere*, San Diego, Academic Press.

Flagan, R. C. (1998). History of electrical aerosol measurements. *Aerosol Science and Technology, 28*, 301-380.

Friedlander, S. K. (2000). *Smoke, dust, and haze: Fundamentals of aerosol dynamics (2nd Ed.)*, New York, Oxford University Press.

Fujii, S., & Kagi, N. (2002). Cleanroom standards and air cleanliness. *Journal of Aerosol Research, 17*, 179-184 (in Japanese).

Hinds, W. C. (1999). *Aerosol technology: Properties, behavior, and measurement of airborne Particles (2nd Ed.)*, New York, Wiley.

Jacob, B., Ritz, B., Gehring, U., Koch, A., Bischof, W., Wichmann, H. E., & Heinrich, J. for the INGA-Study Group. (2002). Indoor exposure to molds and allergic sensitization. *Environmental Health Perspectives, 110*, 647-653.

Kerker, M. (1997). Light scattering instruments for aerosol studies: An historical overview. *Aerosol Science and Technology, 27*, 522-540.

Kitamura, T., Shiomori, T., Fujimura, T., & Suzuki, H. (2005). Allergy (1) Nasal allergy by pollen. *Journal of Aerosol Research, 20*, 54-57 (in Japanese).

Korpi, A., Pasanen, A-L., Pasanen, P., & Kalliokoski, P. (1997). Microbial growth and metabolism in house dust. *International Biodeterioration and Biodegradation, 40*, 19-27.

Lach, V. (1985). Performance of the surface air system air samplers. *Journal of Hospital Infection, 6*, 102-107.

Lapuerta, M., Armas, O., & Gomez, A. (2003). Diesel size distribution estimation from digital image analysis. *Aerosol Science and Technology 37*, 369-381.

Lowenstein, H., Lind, P., & Week, B. (1985). Identification and clinical significance of allergenic molecules of cat origin: Part of the DAS 76 study. *Allergy, 40*, 430-441.

Lowenstein, H., Gravesen, S., Larsen, L., Lind, P., & Schwartz, B. (1986). Indoor allergens. *Journal of Allergy and Clinical Immunology, 78*, 1035-1039.

Martuzevicius, D., Grinshpun, S. A., Reponen, T., Górny, R. L., Shukla, R., Lockey, J., Hu, S., McDonald, R., Biswas, P., Kliucininkas, L., & LeMasters, G. (2004). Spatial and temporal variations of PM2.5 concentration and composition throughout an urban area with high freeway density—the Greater Cincinnati study. *Atmospheric Environment, 38*, 1091-1105.

May, K. R., & Harper, G. J. (1957). The efficiency of various liquid impinger counters in bacterial aerosol. *British Journal of Industrial Medicine, 14*, 287-297.

May, K. R. (1966). Multistage liquid impinger. *Bacteriological Reviews, 30*, 559-570.

Ministry of the Environment, Japan (2005). *Asbestos monitoring manual (revised edition)*, <http://www.env.go.jp/air/asbestos/mon_man_h05.html> Accessed 1 November 2005 (in Japanese).

National Institute of Occupational Safety and Health (2005). *Method #7400 - Asbestos and Other Fibers by PCM*, <http://www.cdc.gov/niosh/nmam/pdfs/7400.pdf/> Accessed 1 November 2005.

Noll, K. E., Fang, K. Y. P., & Watkins, L. A. (1988). Characterization of the deposition of particles from the atmosphere to a flat plate. *Atmospheric Environment, 22*, 1461-1468.

Ohman, J. L., Lowell, F. C., & Bloch, K. J. (1974). Allergens of mammalian origin, III: Properties of a major feline allergen. *Journal of Immunology, 113*, 1668-1677.

Palmgren, U., Ström, G., Malmberg, P., & Blomquist, G. (1986). The Nuclepore filter method: A technique for enumeration of viable and nonviable airborne microorganisms. *American Journal of Industrial Medicine, 10*, 325-327.

Platts-Mills, T. A. E., & Chapman, M. D. (1987). Dust mites: Immunology, allergic disease, and environmental control. *Journal of Allergy and Clinical Immunology, 80*, 755-775.

Schwartz, J., Dockery, D. W., & Neas, L. M. (1996). Is daily mortality associated specifically with fine particles? *Journal of the Air & Waste Management Association, 46*, 927-939.

Swanson, M. C., Agarwal, M. K., & Reed, C. E. (1985). An immunochemical approach to indoor aeroallergens quantitation with a new volumetric air sampler: Studies with mite, roach, cat, mouse, and guinea pig antigens. *Journal of Allergy and Clinical Immunology, 76*, 724-729.

Tai, H. S., Lin, J. J., & Noll, K. E. (1999). Characterization of atmospheric dry deposited particles at urban and nonurban locations. *Journal of Aerosol Science, 30*, 1057-1068.

Tovey, E. R., Chapman, M. D., & Platts-Mills, T. A. E. (1981). Mite faeces are a major source of house dust allergens. *Nature, 289*, 592-593.

van Hout, R., & Katz, J. (2004). A method for measuring the density of irregularly shaped biological aerosols such as pollen. *Journal of Aerosol Science, 35*, 1369-1384.

Yamamoto, N., Fujii, M., Kumagai, K., & Yanagisawa, Y. (2004). Time course shift in particle penetration characteristics through capillary pore membrane filters. *Journal of Aerosol Science, 35*, 731-741.

Yamamoto, N., Kumagai, K., Fujii, M., Shendell, D. G., Endo, O., & Yanagisawa, Y. (2005). Size dependent collection of micrometer-sized particles using nylon mesh. *Atmospheric Environment, 39*, 3675-3685.

Yang, H-H., Cheng, S-K., & Hsieh, L-T. (2004). Characterization of nitrate particulate dry deposition by vacuum-deposited thin film reaction method. *Atmospheric Environment, 38*, 1785-1793.

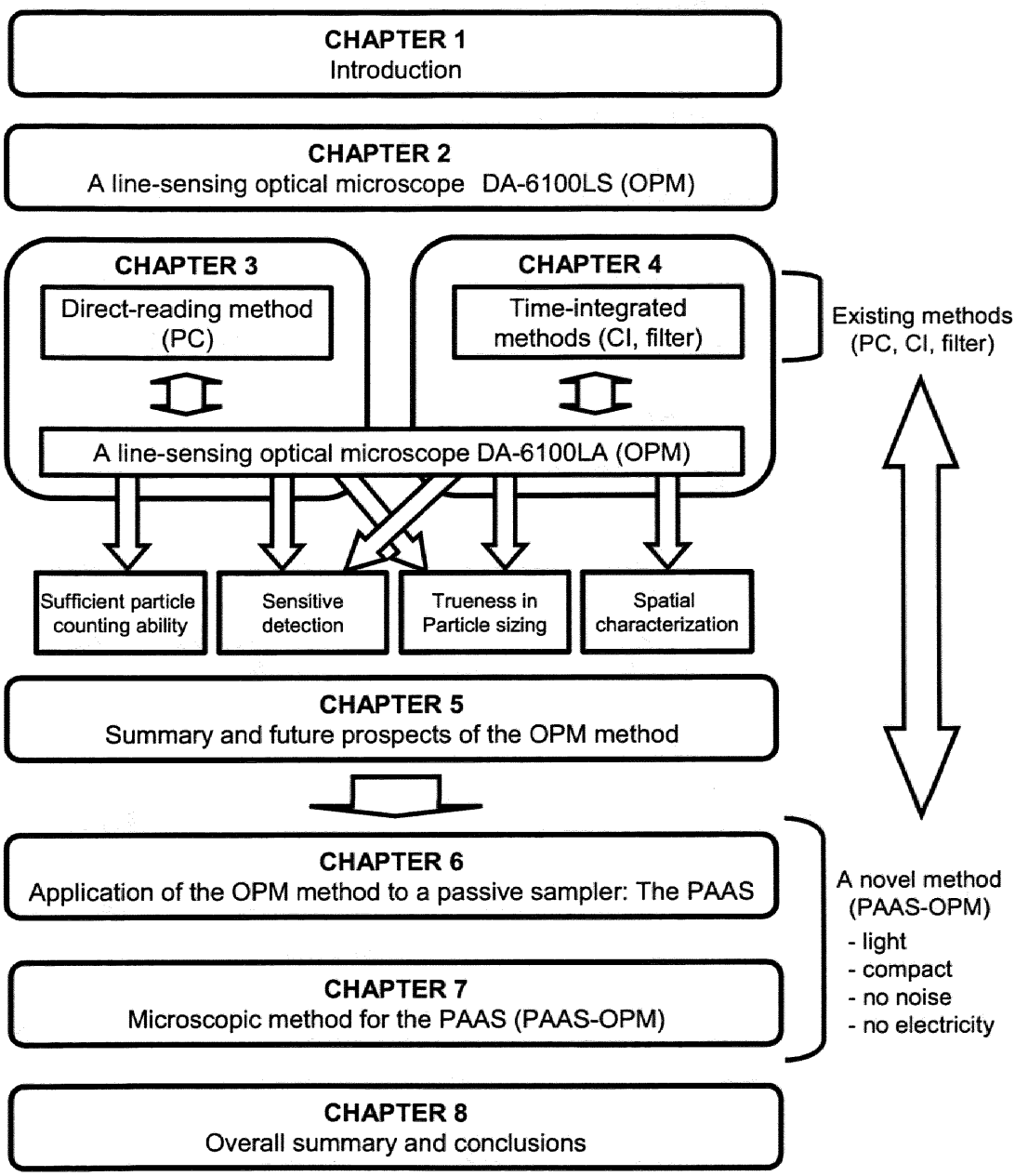

Figure 1.1. Structure of the thesis.

CHAPTER 2.

An optical microscope to analyze airborne coarse particles: Dot Analyzer DA-6100/LS

CHAPTER 2.

An optical microscope to analyze airborne coarse particles: Dot Analyzer DA-6100/LS

CHAPTER 2. An optical microscope to analyze airborne coarse particles: Dot Analyzer DA-6100/LS

2.1. Description of the DA-6100/LS

An optical microscope (OPM), Dot Analyzer DA-6100/LS (Oji Scientific Instruments, Hyogo, Japan) (Figure 2.1), was used in this study. The OPM with a halogen lamp (150 W) as an illuminant takes a form of an incident light method. This OPM is composed of a line-sensor camera (Model SHH-2048; Nippon Electro-Sensory Devices Corp., Osaka, Japan) (Figure 2.2) and a linear actuating slide (Model GLM20; THK Co., Ltd., Tokyo, Japan) (Figure 2.3). Using its line-sensor camera in conjunction with the linear motor actuating slide, the broad range microscopic observation (approximately 5.5 mm × 16.2 mm) is capable at a time (Figure 2.4). The microscope with the objective and relay lenses having magnifying powers of × 2.5 and × 2, respectively, provides a spatial resolution of 2.7 μm. The specifications of the OPM are summarized in Table 2.1. The captured images are imported to the image analysis software, DA-6000, bundled with the OPM to segment the images to black and white pixels and analyze geometric properties of the target substances. The properties that can be analyzed include area, girth, Feret's diameter, shape factor, center of gravity coordinate, Euler number, and so on. The geometric properties that can be calculated by the OPM are summarized in Table 2.2. The OPM has been originally developed to assess inclusion of microscopic foreign substances in the paper sheets during the manufacturing processes as well as evaluate printer's qualities such as line width, jitter,

banding, dot alignment, color resistance, skewness, and so on (Oji Scientific Instruments, 2005).

2.2. Applications of the DA-6100/LS

In this study, the OPM originally used to evaluate the paper sheets have been newly introduced to examine the airborne particles collected on the filters or substrates. Since the OPM can capture a broad microscopic image at a time, the airborne particles collected on a wide range of a filter or substrate are observable in one image. The airborne particles on the filter or substrate are analyzed for their sizes, shapes, numbers and spatial locations. Since the image analysis software can analyze the microscopic images imported from the microscope, a large number of the particles captured on the image can be processed at a time. In consequence, the increase of the observed number of the particles can reduce the statistical error and lower the limit of quantitation in the particle number measurements while the image analysis software can eliminate the human error or bias, and ensure repeatability of the measurements.

The particles collected by filtration and impaction can be characterized by the OPM. For instance, the particles collected on the 47-mm membrane filter for a certain period of time were observed for their size distributions to compare with those characterized by a light scattering method (Chapter 3). In Chapter 4, the particles collected on the impaction substrates can be observed by the OPM, too. The particle depositions on the impactor substrates were observed by the OPM. In particular, the spatial distributions of the particles deposited on the impactor substrates were examined by the OPM. Furthermore, the OPM can be used to analyze the particles passively collected by using its detection sensitivity. Although the number of the particles

collected by the passive methods is generally smaller than that by active methods, the OPM can sensitively detect and quantitate the particles collected by the passive methods. In Chapter 7, the particles collected by the PAAS, a passive sampler for coarse airborne particles, were analyzed by the OPM to evaluate particle collection efficiency of the sampler.

2.3. Summary

Unlike traditional microscopes with stationary sample stages, the OPM with the line-sensor camera in conjunction with the linear motor actuating slide is expected to reduce the statistical error as well as limit of quantitation in the particle concentration measurements since it is easy to assure the measured number of the particles. Moreover, unlike methods using manual counting and sizing of the particles through the microscopes, the image analysis software is expected to eliminate the human error in the particle concentration measurements and ensure repeatability of the measurements.

References

Oji Scientific Instruments (2005). <http://www.oji-keisoku.co.jp/> Accessed 1 November 2005.

Oji Scientific Instruments (2001). Dot Analyzer DA-6000 Operation Manual.

Table 2.1

Specifications of the line-sensing optical microscope

Model	DA-6100/LS
Lens	Objective lens (× 2.5), Relay lens (× 2)
Observation range	5.5 mm × 16.2 mm
Minimum resolution	2.7 μm
Optical system	Reflection method (Incident light method)
Light source	Halogen lamp (150 W)
Line sensor camera	NED SHH-2048
Linear actuating slide	THK GLM20

Table 2.2

Examples of geometrical properties that can be characterized by the image analysis software, DA-6000

Area	Girth	Feret's diameter
Diameter of inscribed circle	Diameter of circumscribed circle	Shape factor
Number of openings	Ellipticity	Center of gravity coordinate
First moment	Second moment	Euler number

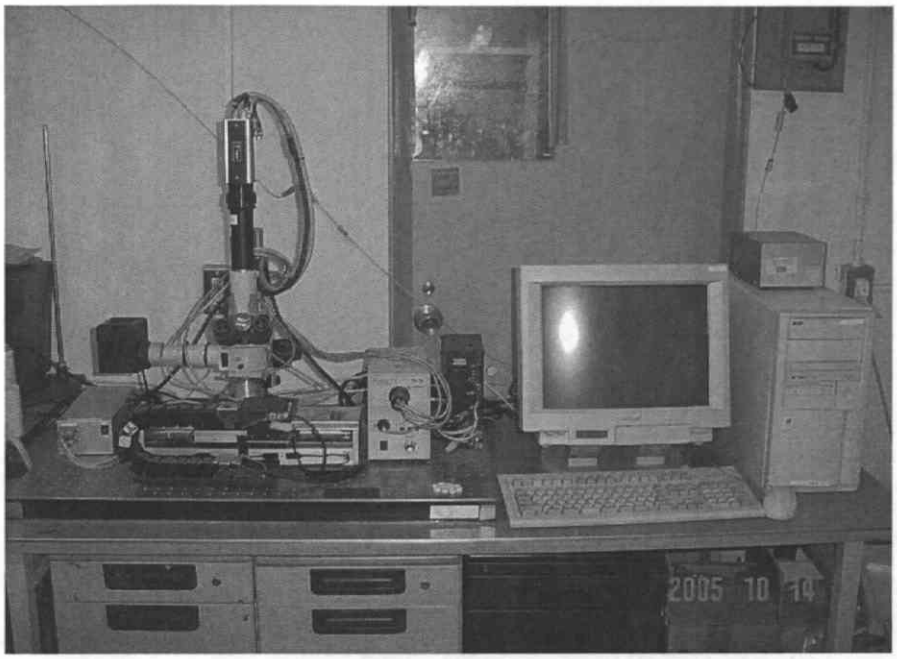

Figure 2.1. Overall image of a line-sensing optical microscope Dot Analyzer DA-6100/LS.

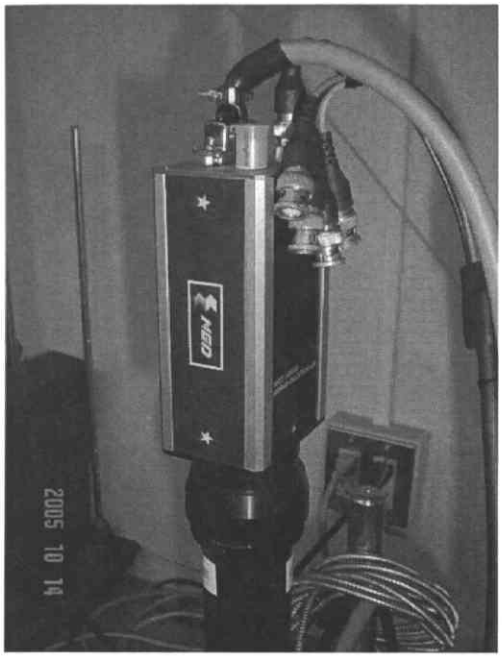

Figure 2.2. A line-sensor camera of the Dot Analyzer DA-6100/LS.

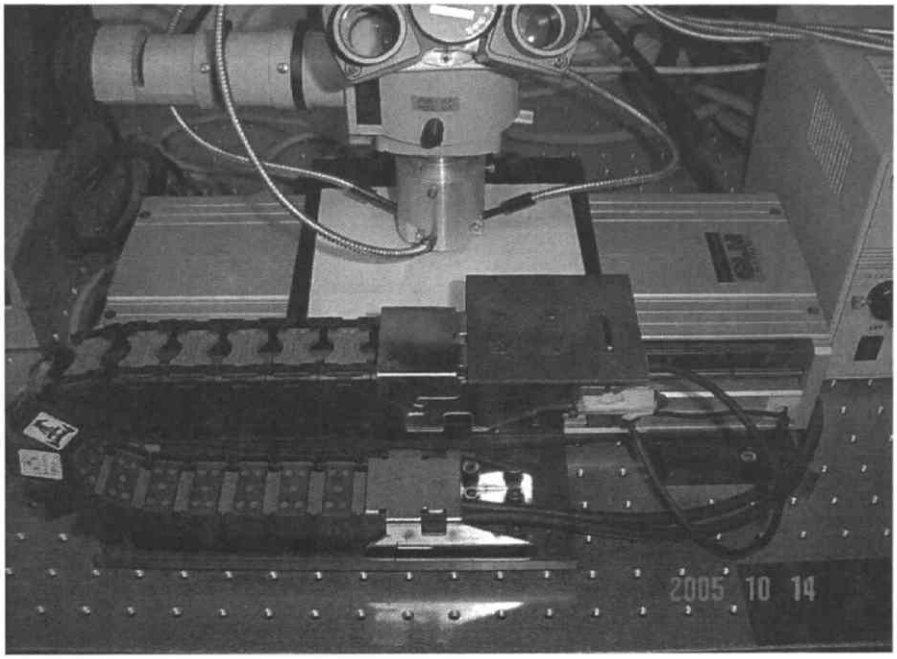

Figure 2.3. A linear actuating slide of the Dot Analyzer DA-6100/LS.

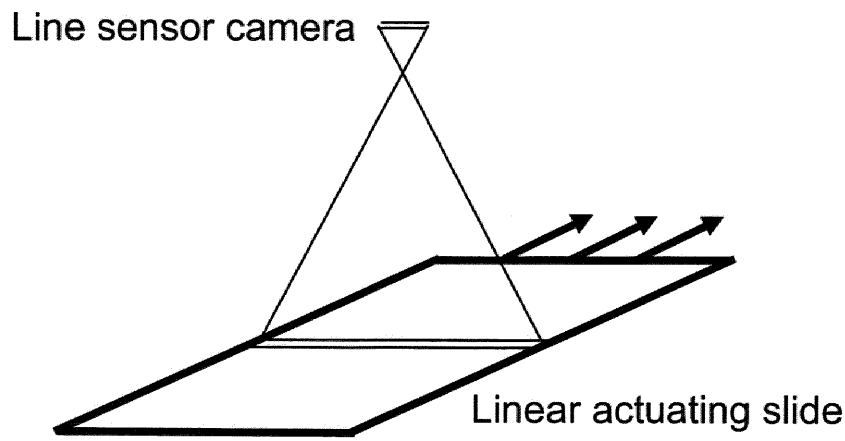

Figure 2.4. Schematic diagram of a line-sensing mechanism.

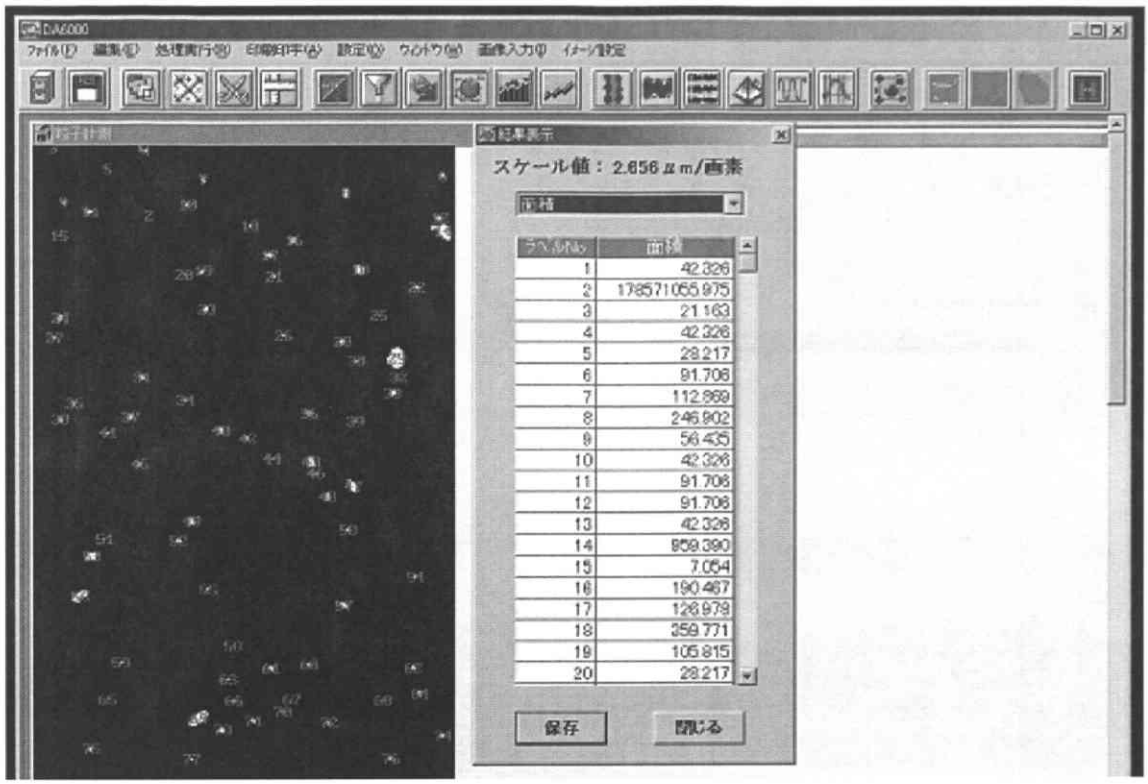

Figure 2.5. Screen image of the image analysis software DA6000.

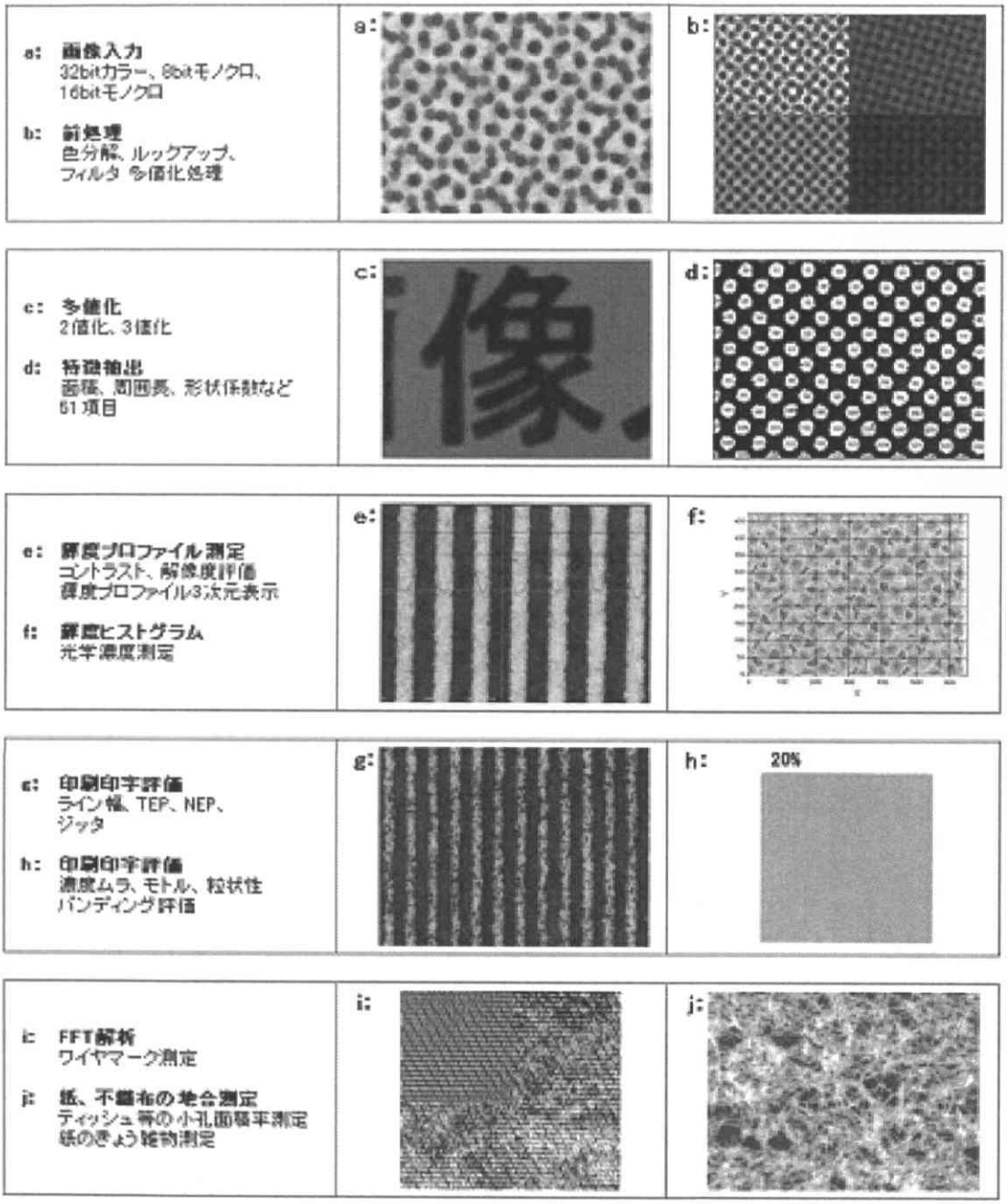

Figure 2.6. Applications of the Dot Analyzer DA-6100/LS (Oji Scientific Instruments, 2005).

CHAPTER 3.
Comparison of the microscopic method with a direct-reading method to measure airborne coarse particles

CHAPTER 3. Comparison of the microscopic method with a direct-reading method to measure airborne coarse particles

3.1. Objectives in the thesis

In this chapter, the OPM method for determining the particle size distributions was evaluated by comparison with an existing direct-reading method, i.e., a light scattering particle counter (PC). In particular, the capability of the OPM method for determining the particle concentrations was validated by crosscheck with the light scattering method. Furthermore, the trueness in particle sizing by the OPM was highlighted by comparison with that by the light scattering method. To validate its trueness in particle sizing, the standard particles of the National Institute of Standards and Technology (NIST) traceable were observed by the OPM.

3.2. General backgrounds

Among many types of aerosol sampling methods, there are two types in general, direct-reading and time-integrated. The direct-reading instruments such as light scattering instruments (Kerker, 1997), time-of-flight monitors (Cheng et al., 1993), condensation nuclei counters (Agarwal & Sem, 1980) and electrical mobility analyzers allow us to measure particle concentrations in a few minutes at sampling sites. Because they instantaneously measure particle concentration, the direct-reading instruments have been widely used, for instance, in occupational hygiene surveys (Hinds, 1999) or clean room (Kalechits et al., 1994) for continuous and periodical

particle detection. Nevertheless, they are occasionally less accurate because they rely their measurements on observing the properties related to size such as light scattering, light absorption, mechanical mobility, or electrical mobility. The time-integrated instruments including filtration and impaction, on the other hand, determine the aerosol concentrations by directly measuring the particle mass collected on the filters or substrates. A filter sample integrates particle mass to provide the average aerosol concentration during a sampling period. Using a microbalance, collected particles are gravimetrically analyzed. Nevertheless, they often require long-term sampling duration to collect sufficient particles for gravimetric analysis although they are generally simple and low-cost.

An instantaneous filter sampling with semi-automated microscopic observation would complement shortcomings of these two types of instruments. A short-term filter sampling, a simple and low-cost method, provides the particle concentrations in a high time resolution. Unlike the direct-reading instruments, the sampled filters are preserved for subsequent microchemical analyses. Although the short-term filtration samplings are often encountered with insufficient particle mass for subsequent gravimetric analysis, we anticipated the microscopic analysis enabled the particle quantification even with extremely small amounts. Moreover, the microscopic investigation can provide additional information such as particle shapes. While the microscopic analyses are generally slow, tedious and often inaccurate due to operational error or bias if the visual investigation was manually performed, we have recently reported the semi computer-automated optical microscope for particle counting (Yamamoto et al., 2002) to overcome these difficulties. Moreover, unlike limited observable areas in the microscopes with the fixed objective lens and slide, a line-sensor

camera with a linear motor actuating slide enabled to capture the particles on a broad area of the substrate at a time.

Although Lapuerta et al. (2003) characterized the size distributions of diesel particles by a digital analysis of the images taken by a scanning electron microscope, they noted the particle numbers measured by their method was not representative of real flowing particle numbers measured by existing direct-reading instruments. The present investigation aims to explore the possibilities of the particle number concentration measurements as well as particle size distribution characterizations by the microscopic observation. The study compared the particle size distributions collected on the filter and measured by the above-mentioned optical microscope (OPM) with those measured by a light scattering particle counter (PC). The concentrations by the OPM and PC were related for each size-fractionated particle group through several collocated measurements. Since the particle sizes identified by the light scattering methods generally differ from the actual geometrical sizes due to difference in scattering properties of the calibration and measured particles, the conceptual aspects of particle size difference characterized between the two different methods are also discussed.

3.3. Methods

The membrane filters (0.45 μm pore size, 47 mm diameter, mixtures of cellulose acetate and cellulose nitrate; Millipore Corp., MA, USA) were used for the filtration samplings. The 3.1-mm interval black grids on the white filter facilitated the concentration calculation by counting the particles on the known fraction of effective filtration surface. The filter paper was placed in an aluminum filter holder with a

stainless steel support (SKC Inc., PA, USA) connected with a silicone tube to a vacuum pump (Model SIP-32L; Sibata Scientific Technology Ltd., Tokyo, Japan), and the sampling flow rate was adjusted at 10 l min^{-1}. A light scattering particle counter (PC) with particle size channels of 10, 20, 30, 50 and 100 μm (Model KC-20, laser diode with wavelength λ of 780 nm, sideway light-scattering method with collection angle θ from 70 to 150 degree; RION Ltd., Tokyo, Japan), for which the particle size calibrations were performed using standard spherical glass bead particles (refractive index; m = 1.56), was collocated with the filtration samplings. The detection limit of the KC-20 Model, defined as spurious count by the PC when monitoring clean air, is less than one particle per 5-min monitoring. Since the monitoring flow rate of the KC-20 Model is 30 l min^{-1}, the detection limit can be calculated less than 0.033 particle l^{-1}. Twelve collocated filtration and PC samplings for durations of 30 to 60 min were taken indoors and outdoors. Indoor and outdoor samplings were taken during August to October 2003 in and out of the sixth floor room of the building (approximately 20 m from the ground level) of the University of Tokyo in Bunkyo-ku, located in the central part of Tokyo. There was no characteristic emission source of coarse micrometer-sized particles around the sampling site. Therefore, the measured particles were expected to be wind blown soil or plant debris suspended near the sampling site. Furthermore, there was no peculiar indoor particulate source during the samplings.

The OPM with a line sensor camera, Dot Analyzer DA-6100/LS (Oji Scientific Instruments, Hyogo, Japan), was used to capture the microscopic images of the particles collected on the filters. Its line sensing mechanism with a linear motor actuating slide enabled broad range observations of target materials (approximately 5.5 mm × 16.2 mm) at a time. Captured images were imported to a graphic software (Adobe

Photoshop 5.0, Adobe System Inc.) to erase image noises, and then segmented into black and white pixels (pixel pitch = 2.7 μm) by an image analysis software, DA-6000, bundled with the OPM (Oji Scientific Instruments, Hyogo, Japan) to process sizes and numbers of collected particles (Figure 3.1). The particle sizing trueness by the OPM was confirmed using black colored polystyrene latex particles with 10 and 100 μm diameters (Duke Scientific Corp., CA, USA) of the National Institute of Standards and Technology (NIST) traceable. The standard black colored particles originally suspended in water were diluted and collected on the membrane filters by suction filtration for the subsequent OPM analysis. To prevent the particle coagulation, the particle suspensions were added with 0.5% (w/w) sodium hexametaphosphate as a dispersant and ultra-sonicated in advance of suction filtration.

3.4. Results and discussion

3.4.1 Particle sizing trueness by the OPM

The particle sizing trueness characterized by observing the standard black colored particles by the OPM is summarized in Table 3.1. The resolution of the digital images taken by the OPM is 2.7 μm. The particle diameters observed by the OPM were defined as particle projected area diameters.

3.4.2 Particle size distributions by the OPM and PC

The particle size distributions by the OPM and PC methods are shown with that by the PC with the particle size conversion (PC*) (Figure 3.2). The procedure of the particle size conversion, required due to difference in scattering properties between calibration and measured particles, will be described in the following section. The

relationship of the particle number concentrations measured through twelve collocated samplings by the PC and OPM are shown in Figure 3.3. The PC measured the particle concentrations by the particle diameter categories of >10, >20, >30 and >50 μm while the OPM counted and measured the particles with continuous particle size. Therefore, the OPM concentrations were calculated based on particle size categories by the PC for comparison. To calculate the OPM concentrations, approximately 500 to 1900 particles with diameters larger than 10 μm were counted on the filter surfaces having areas of 170-420 mm^2.

While the OPM concentrations increased with the PC concentrations, the OPM concentrations tended to be higher than those by the PC. The discrepancy between the PC and OPM size distributions was thought to result from the following reasons: (1) particle overlapping on the filter; (2) counting loss by the PC; (3) underestimate of the particle sizes by the PC. Since the coverage area fractions by collected particles on the filters were relatively small, i.e., 0.04-0.15 %, the particle overlapping was expected to be insignificant to explain the difference between the two size distributions. Furthermore, since the particle counting efficiency by the PC is known to be generally high (e.g., Mäkynen et al., 1982), it was inferred that the particle sizes characterized by the PC were smaller than the actual geometrical sizes.

3.4.3 Particle sizing by the OPM and PC

We first computed the PC response back from the particle diameter measured by the PC, d_{PC}, and looked for the diameter characterized by the OPM, d_{OPM}, that would result in the same PC response from the measured particles. The PC response, or the light intensity received by the instrument, was computed for d_{PC}, the refractive index of

calibration particles, the wavelength and the detection angle range. In computing the angular scattering intensity, we used the Mie theory that was appropriate for particles in sizes comparable to the wavelength. We used the Wiscombe's code for homogeneous spheres (Wiscombe, 1996). Briefly, the diameter adjustment method is represented by the following equation:

$$\int_{70^o}^{150^o} s(m_{cal}, \lambda, d_{PC}, \theta) d\theta = \int_{70^o}^{150^o} s(m_{meas}, \lambda, d_{PC^*}, \theta) d\theta, \qquad (3.1)$$

where s is the angular scattering intensity, m_{cal} is the calibration refractive index (= 1.56), and m_{meas} is the refractive index of the measured particles. Given an estimated m_{meas}, the above equation relates the d_{PC} to the theoretical geometric diameter d_{PC^*}. We linked an array of geometric diameters to the PC response in the same manner but for the urban aerosol with m_{meas} = 1.56-0.087i (Ozkaynak et al., 1985; Hinds, 1999). The values of refractive indices used for this calculation are summarized in Table 3.2. Both the calibration and urban aerosol PC response curves were smoothed over ± 0.17 of common logarithm of diameter, to eliminate their fluctuations insignificant relative to the measurement precision. Interceptions of these two curves at a given light intensity specified corresponding d_{PC} and d_{PC^*} (Figure 3.4). For example, a particle whose diameter was identified as 10.0 μm by the PC turned out to be 19.7 μm geometric large (hence particle size conversion factor C^* of 1.97), as these two curves had an identical light intensity of 11.1. The calculation for the entire PC diameter range shows that the d_{PC^*} were 1.7-2.0 times as large as the corresponding d_{PC} (Figure 3.5). It should be noted that the C^* in Figure 3.5 was based on the assumed particle refractive index of 1.56-0.087i and varied with assumptions of refractive index.

Using the theoretical conversion factors C^*, the particle diameter characterized by the PC was related to the theoretical geometric diameter:

$$d_{PC^*} = C^* \times d_{PC}, \quad (3.2)$$

Therefore, the size ranges by the PC were converted from d_{PC} >10, >20, >30 and >50 μm to d_{PC^*} >20, >36, >54 and >85 μm, respectively, to define the theoretical geometric size ranges by the PC observation. The concentrations recalculated based on these converted size ranges, PC*, are shown in Figure 3.2. The PC* concentrations remain to be equal to the corresponding PC concentrations although the defined particle sizes are different due to the particle size conversion. The relationship of the particle number concentrations through 12 collocated results by the PC* and OPM are shown in Figure 3.6. Some points in the diagram of d_{PC} >50 μm came to zero because there was no particle sized by the OPM within the shifted PC* size range, i.e., d_{PC^*} >85 μm. It is important to note that the current particle size conversion was based on the assumed particle refractive index of 1.56-0.087*i*. Therefore, the converted PC* size ranges on d_{PC^*} could be varied depending on the refractive index assumed. To compare the OPM results based on the variable PC* size ranges, the original PC size ranges as a function on d_{PC} remained to be used although the converted ranges on d_{PC^*} are actually different from the notated values on d_{PC} and varied even in the same diagram depending on the refractive index assumed.

3.4.4 Uncertainties in particle sizing

Since the results could be affected by the uncertainty of the assumed refractive index, the parametric sensitivity to choice of the refractive index was roughly assessed. For the purpose of the sensitivity assessment, we arbitrarily took the uncertainty range of 2 % in the real part, 1.53-1.59, and a factor of two in the imaginary part, 0.044-0.174, (thick dotted lines) as well as the expanded uncertainty range of 4 % in the real part,

1.50-1.62, and a factor of three in the imaginary part, 0.029-0.261 (thin dotted lines). Dotted lines in Figure 3.6 indicate the uncertainty ranges of the regression lines between which the values could take. The lower solid line in the diagram of d_{PC} >50 μm is the two dotted lines coincided. In fact, most of the shift was due to variation in the real part, while the little dependence was shown for the imaginary part over the supermicron diameter range. Overall, the particle number concentrations by the OPM method are lower than those by the PC* within these uncertainty ranges of the refractive index. Provided the above-mentioned assumption of the refractive index was valid, the lower OPM concentrations are probably due to the particles having the similar refractive index of the filter (Table 3.2) that were hardly visible by the OPM. Since the particle counting efficiency by the PC is relatively high, the ratios of the OPM to PC* concentrations approximates the OPM particle counting efficiencies due to the intrinsic OPM limitations. Further investigation is required to examine the measured aerosol speciation to confirm this view.

It should be stressed that refractive index for the observed particles might take values out of the above assumed ranges, depending on their chemical components. For instance, while Marley et al. (2001) obtained the refractive indices of the size-fractionated ambient aerosols ranging 1.41-2.31 for real part and 0.30-0.86 for imaginary part measured at the three cities in the U.S., Ohta et al. (1990) reported the monthly mean values of the imaginary parts of the refractive indices of ambient aerosols in Sapporo, Japan, ranging from 0.024 to 0.047. Since the refractive indices of urban aerosols are found to vary by their sizes (Marley et al., 2001), the use of the single value through the entire size range can cause an additional uncertainty. Particle nonsphericity also disables accurate computation of the PC response, thereby

contributing to uncertainty in the PC method. Thus, while the PC enable quick and easy assessment of aerosol size distribution, its trueness in particle sizing is lowered by our limited knowledge in scattering properties of aerosol species. Meanwhile, the OPM can capture the actual geometries of observed particles without these biases (Table 3.1). This also highlights the advantage in the OPM method particularly for aerosols with unknown compositions.

3.5. Summary

The present study compared the particle size distributions collected on the filter and measured by the OPM with those by the PC to validate the microscopic method for particle size distribution quantification. We found that the microscopic method can measure particle number concentrations with relatively small amount on the filter although the particle size distributions characterized by the OPM and PC methods were different. While the OPM concentrations increased with the PC concentrations, the OPM concentrations tended to be higher. Since diameters identified by the PC differed from those by the OPM due to difference in scattering properties between the calibration and measured particles, we roughly calculated their relationship based on the Mie scattering theory to explain the size distribution difference. The calculation showed the theoretical geometric diameters were 1.7-2.0 times as large as the corresponding d_{PC}. Using these theoretical factors, the particle size ranges by the PC observation were converted, i.e., PC*. The result indicated that the OPM concentrations tended to be lower than those by the PC*. Although the particle counting efficiency by the PC is relatively high, its trueness in particle sizing is lowered by our limited knowledge in the scattering properties of aerosol species. Meanwhile,

the advantage in the OPM method particularly for aerosols of unknown compositions lies in its trueness in particle sizing although the counting efficiency might be of concern.

3.6. Conclusions in the thesis

The ability in the particle concentration measurements was roughly assured for the OPM method. Although the microscopic methods are generally performed manually and the methods for determining particle size distributions are known to be tedious and less precise, the OPM used in this research could overcome these difficulties by means of the image analysis software and the line-sensor camera in conjunction with the linear motor actuating slide. These features could reduce the time required to analyze sufficient number of the particles for precise particle concentration measurements. In general, 20 to 30 minutes of the time were required to analyze the particles collected on a filter surface with observed areas of A = 170-420 mm^2 although the required time was dependent on the surface areas observed. In consequence, statistical error in particle size distribution measurements was reduced by the OPM. Indeed the concentrations obtained by the OPM were quite consistent with those by an existing direct-reading method, i.e., the light scattering particle counter, indicating the particle concentration measurements by the OPM was comparable to that by the light scattering method although the size distributions by the light scattering method were located in the finer side. The discrepancy in the particle sizes characterized by both methods was expected due to scattering properties of the measured particles. In terms of particle sizing trueness, the OPM is more advantageous since it permits direct measurement of the particle size and shape. It should be stated that use of the image

analysis software was particularly useful to reduce the time required for particle sizing. Even though it might not take much time to count the number of the particles, it is extremely tedious to manually size the particles. Although we did not use a manually operated microscope to compare the particle size distribution results with those by the OPM, it was obvious that the time required to analyze was significantly shortened by the computer-based OPM. In this regard, computer-based analyses are undoubtedly essential to determine size distributions of the particles.

References

Agarwal, J. K., & Sem, G. J. (1980). Continuous flow, single-particle-counting condensation nucleus counter. *Journal of Aerosol Science, 11*, 343-357.

Cheng, V. S., Barr, E. B., Marshall, I. A., & Mitchell, J. P. (1993). Calibration and performance of an API aerosizer. *Journal of Aerosol Science, 24*, 501-514.

Hinds, W. C. (1999). *Aerosol technology: Properties, behavior, and measurement of airborne particles (2nd Ed.)*, Wiley, New York.

Kalechits, V. I., Kirsch, A. A., Kulibaba, V. I., Maslakov, O. Y., & Pavlov, Y. V. (1994). 15.P.10 Aerosol control and monitoring system LADA. *Journal of Aerosol Science, 25*, Suppl. 1, S207-S208.

Kerker, M. (1997). Light scattering instruments for aerosol studies: an historical overview. *Aerosol Science and Technology, 27*, 522-540.

Lapuerta, M., Armas, O., & Gomez, A. (2003). Diesel size distribution estimation from digital image analysis. *Aerosol Science and Technology, 37*, 369-381.

Mäkynen, J., Hakulinen, J., Kivistö, T., & Lehtimäki, M. (1982). Optical particle counters: Response, resolution and counting efficiency. *Journal of Aerosol Science, 13*, 529-535.

Marley, N. A., Gaffney, J. S., Baird, C., Blazer, C. A., Drayton, P. J., & Frederick, J. E. (2001). An empirical method for the determination of the complex refractive index of size-fractionated atmospheric aerosols for radiative transfer calculations. *Aerosol Science and Technology, 34*, 535-549.

Ohta, S., Murao, N., & Moriya, T. (1990). Evaluation of absorption properties of atmospheric aerosols at solar wavelengths based on chemical characterization. *Atmospheric Environment, 24*, 1409-1416.

Ozkaynak, H., Schatz, A. D., Thurston, G. D., Isaacs, R. G., & Husar, R. B. (1985). Relationship between aerosol extinction coefficients derived from airport visual range observations and alternate measures of airborne particle mass. *Journal of the Air Pollution Control Association, 35*, 1176-1185.

Wiscombe, W. J. (1996). Mie scattering calculations: advances in technique and fast, vector-speed computer codes. NCAR/TN-140+STR, NCAR TECHNICAL NOTE June 1979 (edited/revised August 1996). ftp://climate.gsfc.nasa.gov/pub/wiscombe/.

Yamamoto, N., Fujii, M., Endo, O., Kumagai, K., & Yanagisawa, Y. (2002). Broad range observation of particle deposition on greased and non-greased impaction surfaces using a line-sensing optical microscope. *Journal of Aerosol Science, 33*, 1667-1679.

Table 3.1

Analytical results of the standard black colored polystyrene latex particles measured by the present OPM method

	Particle diameter (μm)	
Measured [a]	10.1 ± 6.6 (n = 1568)	99.0 ± 9.0 (n = 16)
Information value [b]	10.0 ± 0.1	100.0 ± 1.7

[a] Mean and 1 standard deviation.

[b] Certified value.

Table 3.2

Refractive index

Material	Refractive index
Air	1.00028
Urban aerosol (avg.) [a]	1.56-0.087*i*
Glass (standard particles) [b]	1.56
Membrane filter [c]	1.51

[a] Ozkaynak et al. (1985); Hinds (1999).

[b] Manufacturer of the particle counter.

[c] Mixture of cellulose acetate and cellulose nitrate, manufacturer of the filter.

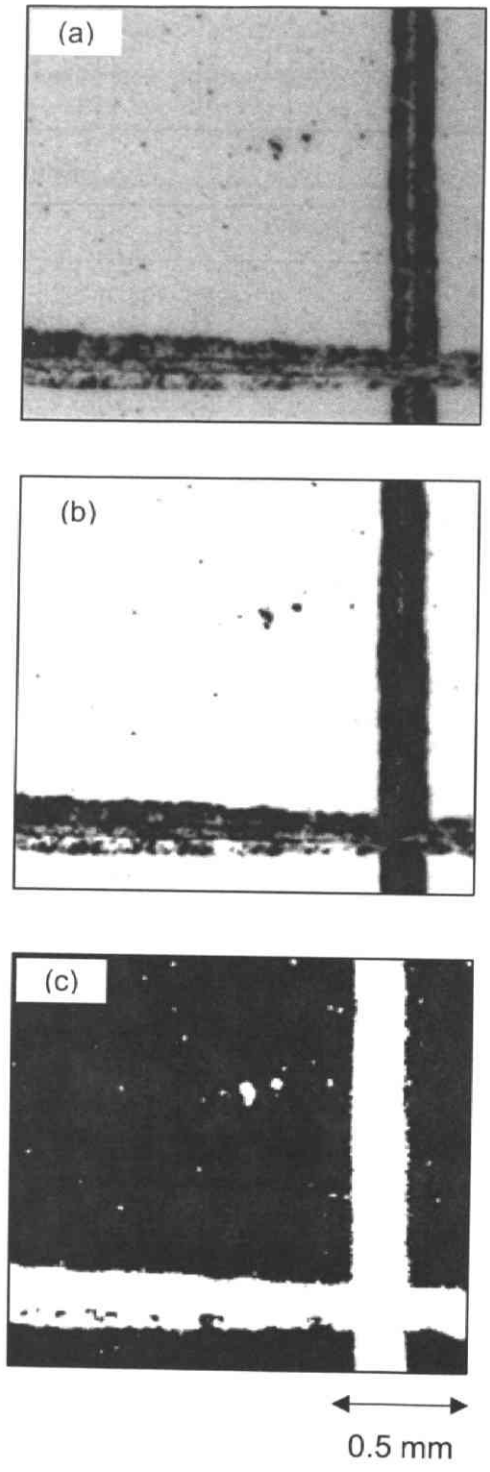

Figure 3.1. A captured image (a), imported to a graphic software to erase image noises (b), and segmented into black and white pixels by an image analysis software (c).

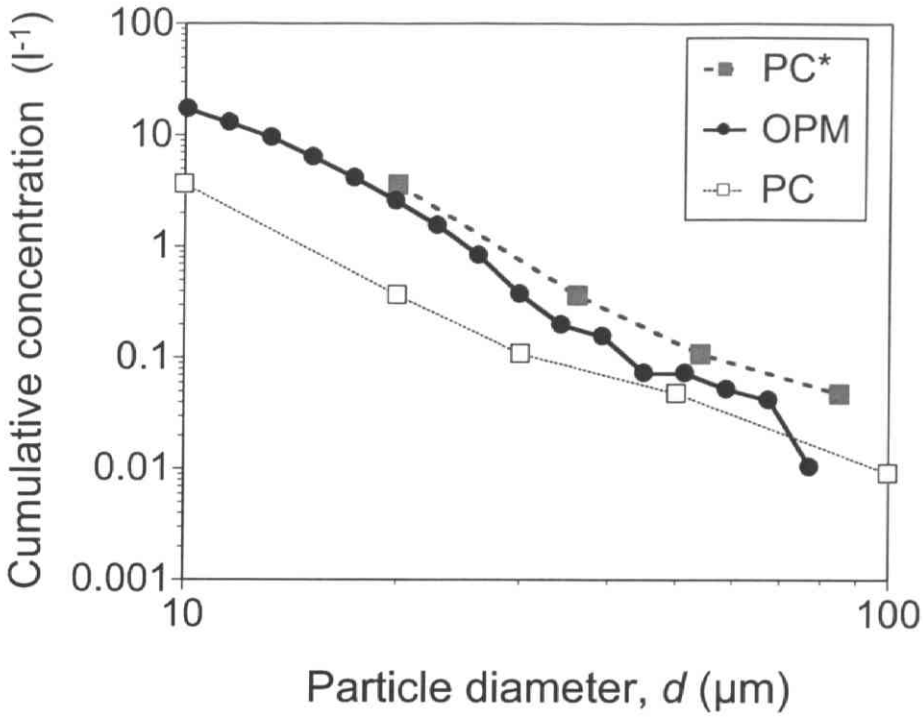

Figure 3.2. Particle size distributions by the OPM, PC and PC*. Concentrations are accumulated from the largest to smaller particle size fractions.

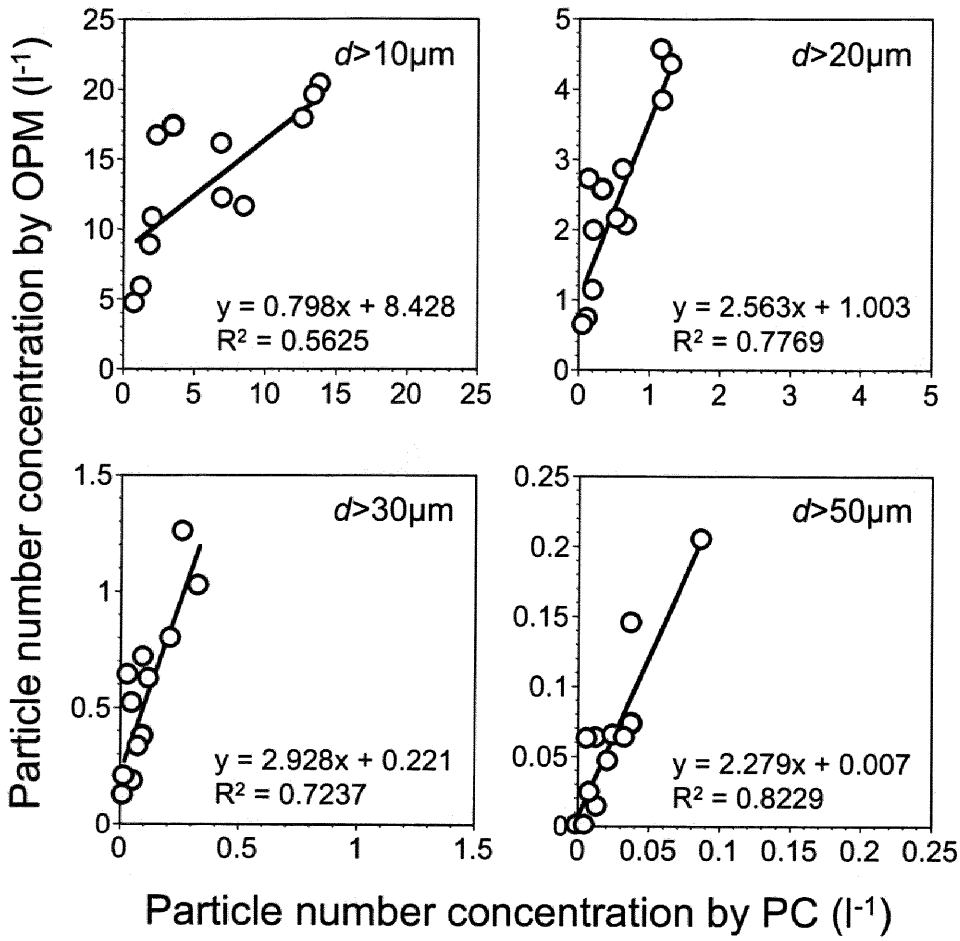

Figure 3.3. Particle number concentrations by the PC and OPM.

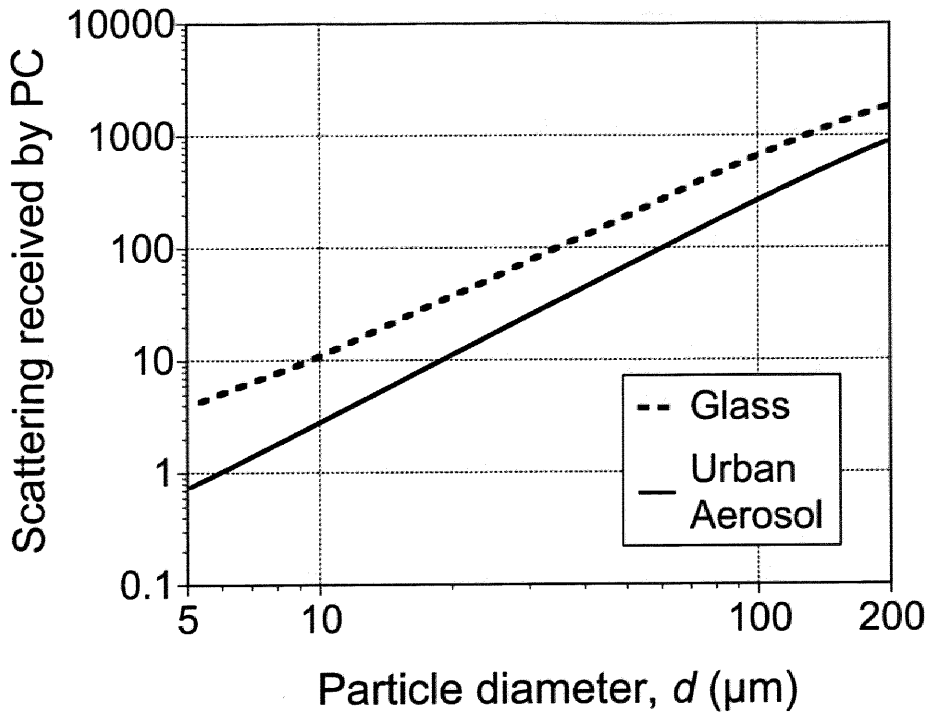

Figure 3.4. Simulated PC responses to glass (m_{cal} = 1.56) and urban aerosols (m_{meas} = 1.56-0.087i).

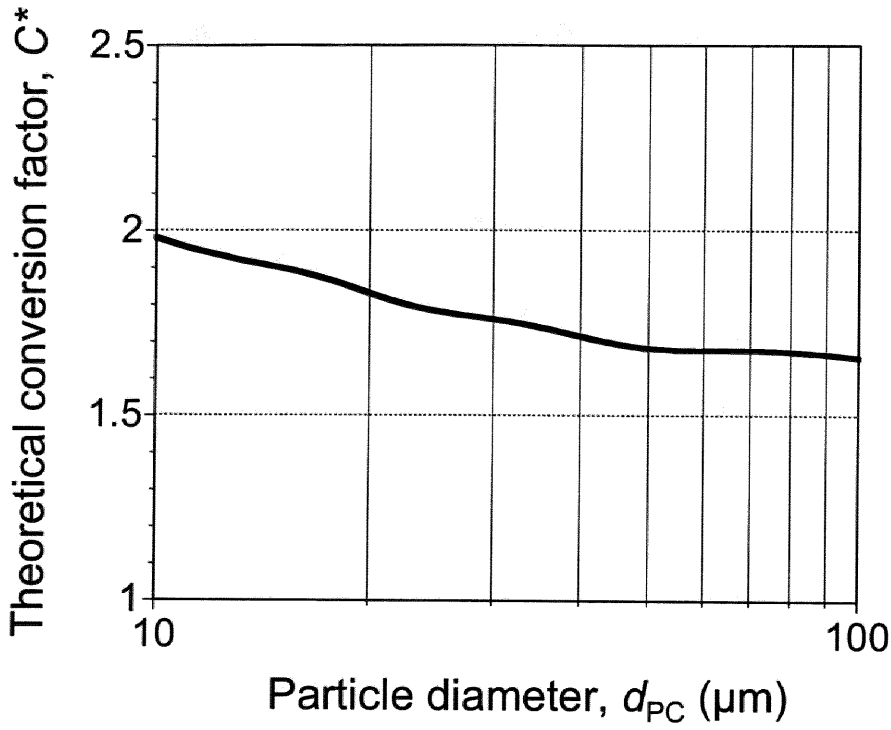

Figure 3.5. Theoretical factors for particle size conversion. Glass (m_{cal} = 1.56) and urban aerosols (m_{meas} = 1.56-0.087i) were assumed for calibration and measured particles, respectively.

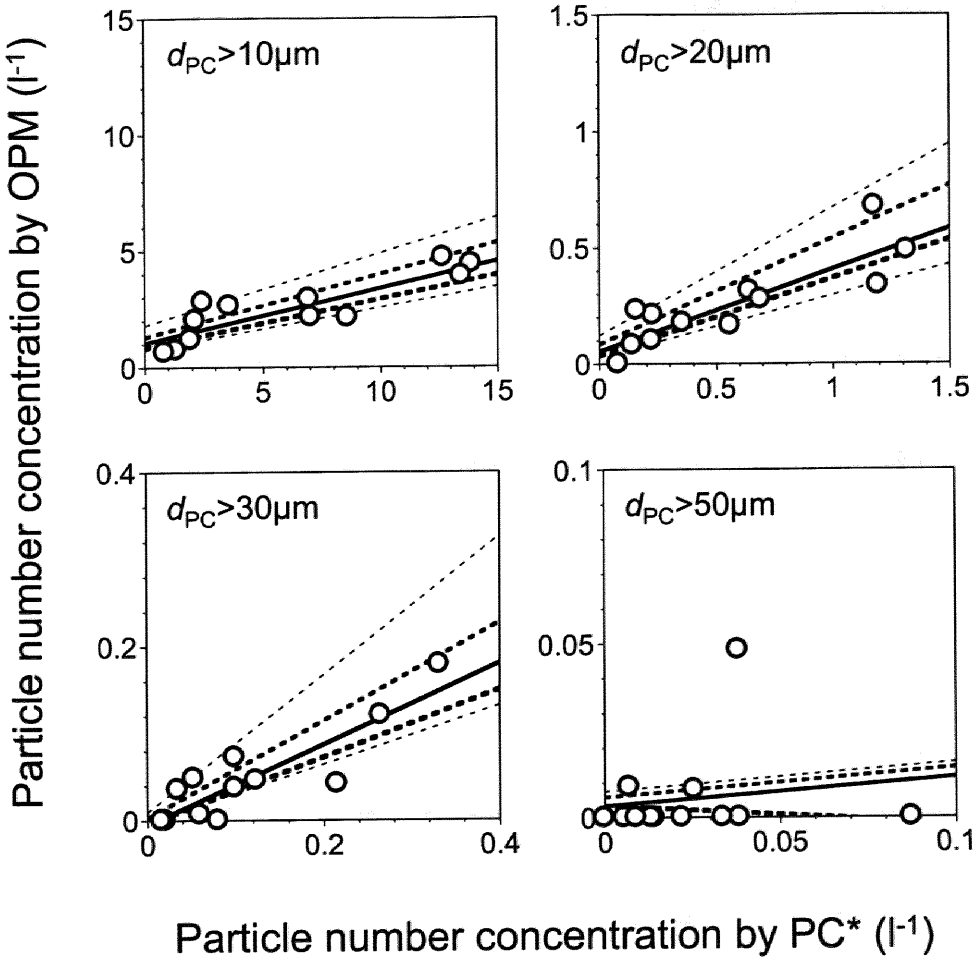

Figure 3.6. Particle number concentrations by the PC* and OPM. Thin and thick dotted lines indicating roughly estimated uncertainty ranges of the assumed refractive index specified in text.

CHAPTER 4.
Comparison of the microscopic method with existing time-integrated methods to measure airborne coarse particles

CHAPTER 4. Comparison of the microscopic method with existing time-integrated methods to measure airborne coarse particles

4.1. Objectives in the thesis

Unlike the direct-reading methods such as the light scattering particle counter, airborne particles are collected and retained on the collection substrates in the cascade impactors (CI). Therefore, the particles collected by the CI can be subsequently analyzed for chemical constituents by a variety of analytical methods. Furthermore, since the particles are size-fractionated and collected by means of particle inertia in the CI, the size distributions of chemical constituents can be analyzed. Nevertheless, the capability of the particle size fractionation is known to be deteriorated by particle bounce and/or reentrainment on the impactor substrates due to accelerated air. In this chapter, the particles collected on the impactor substrates were observed by the OPM to suggest issues related to the particle losses from the impactor substrates. Moreover, the sensitivity of the OPM was emphasized by roughly calculating the masses of the particles collected on the impactor substrates identified by the OPM. To strengthen the hypothesis that the microscopic methods are more sensitive than existing direct-weighing methods using the microbalances, time-course accumulations of the particles on a filter were investigated by both microscopic and direct-weighing methods and compared for their detection sensitivities.

4.2. General backgrounds

Impactors use the principle of inertia to collect and/or separate airborne particles based on their Stokes numbers. In the space between the nozzle exit and impactor plate, accelerated particles tend to continue in a straight line and eventually impact on the flat impaction plate due to their inertia while the air streamlines bend sharply. Although large particles, i.e., those with Stokes numbers larger than a critical value, tend to be unable to follow the air streamlines due to their inertia, small particles can follow them. Using this mechanism, the cascade impactors (CI), samplers with impactor stages in series, have been widely used to measure the particle size distributions because of their capability to separate polydisperse airborne particles based on inertial classification. Many types of the CI including the Lundgren impactor, Andersen sampler, Mercer impactor, and the micro-orifice uniform deposit impactor (MOUDI) (Marple et al., 1987; Marple et al., 1991) have been developed for aerosol sampling over the past few decades.

In inertial impactors, large, dense and solid particles often bounce on the impaction plates because of their kinetic energy of rebound (Dahneke, 1971). Since the nozzle velocities become greater in subsequent stages, the particles once bounced are likely to continue to bounce until they reach the final stage of the CI, typically an afterfilter. In addition to bounce, the particle reentrainment, i.e., blow off of the particles by a jet with sufficient force to overcome adhesive forces between the particles and impaction surface, is also important (Hinds, 1999). Corn & Stein (1965) used various sizes of glass beads to investigate particle reentrainments in relation to the particle sizes and bulk air velocities. In their study, the particle reentrainments were increased for larger particles and with greater air velocities. For these reasons, the

particle bounce and reentraiment errors can be often significant in the size distribution measurements by the CI (Dzubay et al., 1976; Cheng & Yeh, 1979). It is known that surface roughness of substrate materials, types of coating materials, particle size, nozzle velocity, and solidity and hardness of the particles play important roles on particle bounces and reentrainments (Rao & Whitby, 1978a, b; Reischl & John, 1978; Ellenbecker et al., 1980; Hinds et al., 1985; Turner & Hering, 1987; Newton et al., 1990; Chang et al., 1999). Although some impaction substrates such as quartz fiber have relatively soft surfaces which reduce particle bounce and reentrainment due to some partial entrainment of the impinging air streamlines on the impaction substrate, smooth and solid surface substrates such as aluminum foil or Teflon PTFE filters result in the particle loss from the target stage and contamination of the subsequent stages by bounced or re-entrained particles. The most commonly used method to reduce particle bounces and reentrainments is application of high viscosity grease on impaction surfaces (Rao & Whitby, 1978a, b; Turner & Hering, 1987). Nevertheless, the greasing materials may interfere for the chemical analyses. While coating with oil or grease is essential if elimination of large particles is only the purpose of impaction, it is not always applicable especially in the CI for which all the stages are normally intended for subsequent analyses.

To investigate particle loss due to bounces and/or reentrainments, monodisperse fluorescent polymer microspheres were often used in the laboratory experiments (Wall et al., 1990; Chang et al., 1999). The amounts of traceable fluorescent particles collected on the impaction surfaces and afterfilter were subsequently analyzed by fluorescence detectors to compare the mass balance of particles on each medium. Furthermore, this method could investigate the wall loss of

the particles by washing sampler's walls to extract them (Chang et al., 1999). Provided the greased impaction surfaces could completely prevent from the particle bounce and reentrainment, afterfilters loaded on the downstream of each greased and non-greased impaction plate in collocated samplers were weighed to compare the amounts of particles even though the wall loss of particles could not be considered in this method.

Many methods have been attempted to quantitate the particle bounces and reentrainments on the impaction substrates. To our knowledge, however, no study has ever been conducted to visually investigate an entire area of the particle deposit created by an individual acceleration nozzle of an inertial impactor. Since the microscopic investigation of the particles is normally performed manually, it is slow, tedious and often inaccurate due to operator error or bias (Hinds, 1999). Furthermore, the scope of observable area is quite limited in the optical microscopes with the fixed objective lens and slide. To overcome these difficulties, a computer-automated optical microscope (OPM) combined with a line-sensor camera in conjunction with a linear motor actuating slide was introduced to capture an entire image of the particle deposit. The OPM was used to characterize the entire image of the particle deposit on an impaction plate generated by an individual acceleration nozzle of a CI, and investigate possible mechanisms of particle bounce and reentrainment by comparing spatial patterns of the particles deposited on the greased and non-greased Teflon impactor plates. The OPM could investigate particle bounce and reentrainment at real sampling situations, as opposed to laboratory-based experiments using monodisperse aerosols, and identify the size portion of bounced and/or re-entrained particles for a given impactor stage.

4.3. Methods

4.3.1. Impaction experiment

In this study, a high volume Andersen sampler (Model AH-600, Sibata Scientific Technology Ltd., Tokyo, Japan) was used as a CI. Although the quartz fiber substrates, designed for this sampler were commercially available, the PTFE Teflon substrates with 1 mm thickness were used as impactor substrates to imitate the sampling situations where the smooth substrates such as aluminum foil or Teflon PTFE filter are employed in an inertial impactor. Furthermore, white Teflon substrates are convenient to observe the particles by an optical microscope because of its contrast with dark color airborne particles composed mostly of black carbon, typical of the Tokyo area (Kaneyasu, 1998). The Teflon plates were cut into approximately 1 cm × 1 cm pieces and were placed right beneath the nozzle exits from the upper stages of the CI. The high volume Andersen sampler was used because the large stage area (approximately 30 cm of diameter) and sufficient space among each nozzle hole on a sampling stage enabled to place 1 cm × 1 cm pieces of Teflon substrates (Figure 4.1). The numbers of the nozzles, air velocities and diameters of nozzles of each stage are summarized in Table 4.1.

To investigate the particle bounce and reentrainment, the numbers of the deposited particles on the non-greased (NG) and greased (G) Teflon substrates were compared. Since particle bounce and reentrainment were expected to occur mostly on the inlet stage which collects the large particles with sufficient energy to bounce and/or re-entrain, the experiments were performed on the inlet stage, i.e., the stage to collect the particles larger than 7 μm in aerodynamic diameter, d_a. Both the greased and non-greased substrates were collocated on the impactor stage (Figure 4.1). The

three-quarters of the stage were covered with the quartz fiber filter while the remaining one-quarter was reserved for 12 Teflon substrates. Twelve Teflon substrates in total including 6 greased and 6 non-greased surfaces were placed immediately beneath the exits of 12 acceleration nozzles. The Teflon substrates were directly attached on the steel surface of the impactor stage by double-sided tape. In this experiment, high-vacuum silicone grease (Dow Corning Asia Inc., Kanagawa, Japan) dissolved in acetone was applied onto the impaction surfaces for the greased Teflon substrates. The air samplings were conducted on the roof of the building of the National Institute of Public Health, Tokyo, Japan on May 14 and August 7, 2002. Two samplings were performed to observe the effect of the relative humidity (RH) on the particle bounce and/or reentrainment. Ambient sampling conditions including the temperature and RH are shown in Table 4.2. In these experiments, a sampling flow rate was adjusted at 566 l min^{-1} as specified for the sampler, and the air samples were taken for 90 and 45 min for May 14 and August 7 samplings, respectively.

An optical microscope with a line sensor camera (OPM) (Model DA-6100/LS; Oji Scientific Instruments, Hyogo, Japan) was used to examine the particles collected on the greased and non-greased Teflon impaction substrates. Using its advantage of line sensing mechanism, accomplished with its linear motor actuating slide, to capture broad ranges of target materials, an entire area of the particle deposit created by each individual acceleration nozzle was observed. The captured images were segmented into black and white pixels (pixel pitch = 2.7 μm) by the image analysis software, DA-6000, bundled with the optical microscope (Oji Scientific Instruments, Hyogo, Japan) to process sizes, numbers and locations of the deposited particles.

4.3.2. Filtration experiment

To demonstrate detection sensitivity of the OPM, the time-course accumulations of the particles on a filter were investigated by both of the microscopic and direct-weighing methods. The Institute for Occupational Medicine (IOM) sampler (SKC Inc., PA, USA) connected to a portable pump (MP-Σ500; Sibata Scientific Technology Ltd., Tokyo, Japan) was used to collect the particles on the mixed cellulose ester membrane (MCE) filter. A sampling flow rate was adjusted at 2 l min^{-1} as instructed by the manufacturer. Airborne particles accumulated on the 25-mm filter were quantitated at each elapsed time of the sampling, i.e., 15, 30, 60, 90, 120, 180 and 300 min. Air samplings were taken in January 2006 out of the sixth floor room of the building (approximately 20 m from the ground level) in the central part of Tokyo.

An analytical balance (Model AG204; readability 0.1 mg; Mettler Toledo Inc.) was used as a direct-weighing method. The filter was weighed before and after each elapsed time to measure the accumulated particle masses on the filter. A blank filter was also weighed whenever the sampled filter was analyzed. Filter weighing was repeated three times to define the measurement precision by the analytical balance. The weighing results were corrected for a blank filter. Meanwhile, the OPM was used to enumerate the particles on the same filter that was analyzed by the analytical balance. The particles collected on the filter surface with an area of 50 mm^2, i.e., approximately 18 % of the effective filter surface, were observed by the OPM to quantitate the number of collected particles on a unit area. In this experiment, the particles with diameters larger than 10 μm were analyzed by the OPM. To characterize the measurement precision by the OPM, the microscopic analyses were repeated 3 times by observing 3 different 50-mm^2 surfaces of the same filter.

4.4. Results and discussion

4.4.1. Particle bounce in the CI

The microscopic images of the particle deposit on the greased and non-greased Teflon impaction substrates are shown in Figure 4.2. The particle numbers and size distributions based on their projected area diameters, d_{PA}, on the greased and non-greased Teflon impaction substrates at 54 and 84 % RH are summarized in Tables 4.3 and 4.4. The results indicated variability of the particle numbers collected on each type of the impaction surfaces was small among the nozzles ($N = 245 \pm 24$ and 119 ± 18 for the greased and non-greased substrates at 54 % RH, and $N = 488 \pm 53$ and 368 ± 77 at 84 % RH, respectively). Furthermore, the particle size distributions on each type of the substrates were also consistent among the nozzles, ranging 13.8-15.8 and 11.2-13.4 μm of geometric mean particle diameters for the greased and non-greased impaction substrates at 54 % RH, and 11.8-13.0 and 10.8-11.7 μm of the diameters at 84 % RH, respectively. Geometric standard deviations (GSD) of the particle size distributions were 1.6-1.7 and 1.6-1.8 for the greased and non-greased substrates at 54 % RH, and 1.6-1.7 and 1.6-1.7 at 84 % RH, respectively. In Figures 4.3 and 4.4, the size distributions of the particles collected on the greased and non-grease substrates are shown with calculated frequency of lost particles defined as differences between particle numbers on the greased and non-greased substrates. The size distributions in Figures 4.3 and 4.4 were obtained from the ambient air of 1.0 and 0.5 m^3 collected through 6 nozzles (total 300 nozzles/stage) with flow rate of 566 l min^{-1} for 90 and 45 min, respectively. The results indicated the larger particles were selectively lost from the non-greased impaction substrates.

In these experiments, approximately 65 % of the particle mass and 50 % of the

particle number were lost from the non-greased substrates at 54 % RH, while 45 % by mass and 25 % by number were underestimated at 84 % RH, respectively, assuming all the particles were spheres with uniform density. These findings suggest errors in the size distribution measurements due to the particle bounces and/or reentrainments affected to a higher degree based on the mass concentrations rather than on the number concentrations. Moreover, the particle loss due to bounce and/or reentrainment was found to occur more significantly at lower RH, which has been studied by numerous investigators (Owens, 1923; Winkler, 1974; Stein et al., 1994; Vasiliou et al., 1999). It should be stated the size distributions in Tables 4.3 and 4.4 and Figures 4.3 and 4.4 were based on particle projected area diameters. Therefore, the distributions might be distorted by the deformation of particles at the moment of impaction. Since the particle deformation energy may be altered with application of the greasing materials, the particle size distributions on greased and non-greased substrates might be affected differently. The effect of the application of the grease on the particle deformation is an issue that requires further investigation using three dimensional profile microscopes for instance. Nevertheless, the result could confirm the reproducible collection characteristics among nozzles even though the application of the grease increased the collection efficiency and altered the size distribution of the collected particles to the larger side.

The particle deposit patterns were characterized along the distance from the central point of the particle deposit, i.e., a point at which the jet centerline intersected the impaction substrate. Since it was inaccurate to externally determine the center of particle deposit using micrometers, the point was defined based on the spatial distribution of the deposited particles on the impaction plane. Since the particle